CHARLES UNIVERSITY

FACULTY OF PHARMACY IN HRADEC KRÁLOVÉ

Department of Biophysics and Physical Chemistry

IN VITRO STUDY OF ^{99m}Tc-LABELLED PEPTIDE TARGETED ON VEGF RECEPTOR

Diploma thesis

Supervisor: Mgr. Pavel Bárta, Ph.D

Hradec Králové, 2024 **Amir Mohammad Nazarzadeh**

Acknowledgment

I would like to express my deepest gratitude to my supervisor, Mgr. Pavel Bárta, Ph.D., for his unwavering support and guidance during the course of my research. His expertise, mentorship, and dedication have been invaluable in shaping this thesis. I would also like to extend my heartfelt thanks to my parents for their constant encouragement, love, and belief in my abilities. Their unwavering support has been a source of strength and motivation throughout this academic journey.

I declare that this work is my original author's work. All literature and other sources, from which I drew during the processing, are listed in the list of used literature and are properly cited in the work. The work was not used to obtain any different or the same degree.

In Hradec Králové, 26 August 2024

ABSTRACT

Diploma thesis title: **In vitro study of ^{99m}Tc-labelled peptide targeted on VEGF receptor**

Author:**Amir Mohammad Nazarzadeh**

Supervisor: Mgr. Pavel Bárta, Ph.D

Charles University, Faculty of Pharmacy in Hradec Králové

Department of Biophysics and Physical Chemistry

Background: Recent advances in tumour imaging and therapy have highlighted the potential of radionuclide-labelled biologically active molecules specificaly targeting tumour-associated receptors. Therefore, the presented study aimed to develop and evaluate an 18-amino acid peptide labelled with technetium-99m ([^{99m}Tc]Tc-MA peptide) as a possible tool for imaging of cancer processes positive on the VEGF receptor type 2 (VEGFR2), a critical component in tumour angiogenesis.

Methods: The MA peptide was synthesized by extending a previously reported 15-amino acid peptide with three additional amino acids (lysine, aspartic acid, and cysteine) to enhance its water solubility and facilitate radiochemical modification. After labelling the MA peptide with technetium-99m and its purity control, it was tested for stability in mouse serum. Then human glioblastoma cell line (U-87 MG) was used for *in vitro* internalization, saturation, and competition study with the prepared [^{99m}Tc]Tc-MA peptide.

Results: The optimalization of radiolabelling process achieved 100% radiochemical purity, and the [^{99m}Tc]Tc-MA peptide demonstrated high stability in mouse serum, with a biological half-life exceeding 180 minutes. In addition, [^{99m}Tc]Tc-MA peptide showed a good and steady rise in internalization of radioligand and the majority of receptor-bound [^{99m}Tc]Tc-MA peptide was internalized after 90 min. Moreover, a strong binding affinity of [^{99m}Tc]Tc-MA peptide to VEGFR2 was observed, with the found values of equilibrium dissociation constant K_D = 103.2 nM and inhibitory concentration IC_{50} = 3.75 μM.

Conclusion: The above summarized results indicate that the [^{99m}Tc]Tc-MA peptide could be considered a promising agent for VEGFR2-targeted tumour imaging, warranting further investigation in *in vivo* preclinical studies.

Keywords: angiogenesis, peptide, technetium-99m, tumour imaging, SPECT, VEGFR2

ABSTRAKT

Název diplomové práce: **In vitro studium ^{99m}Tc-značeného peptidu cíleného na VEGF receptor**

Autor práce:**Amir Mohammad Nazarzadeh**

Školitel: Mgr. Pavel Bárta, Ph.D

Univerzita Karlova, Farmaceutická fakulta v Hradci Králové

Katedra biofyziky a fyzikální chemie

Teorie: Nedávné pokroky v oblasti zobrazování a léčby nádorů zdůraznily potenciál radioaktivně značených biologicky aktivních molekul zaměřených na konkrétní receptory spojené s nádory. Předkládaná studie proto měla za cíl vyvinout a zhodnotit 18-aminokyselinový peptid značený techneciem-99m ([^{99m}Tc]Tc-MA peptid) jakožto vhodný nástroj pro zobrazení nádorů exprimujících VEGF receptor typu 2 (VEGFR2), který je důležitým faktorem pro angiogenezi tumorů.

Metody: MA peptid byl syntetizován dle dříve publikované struktury 15-aminokyselinového peptidu s prodloužením o tři další aminokyseliny (lysin, kyselina asparagová a cystein) pro zvýšení jeho rozpustnosti ve vodě a usnadnění radiochemické modifikace. Po značení MA peptidu techneciem-99m a kontrole radiochemické čistoty byla testována jeho stabilita v myší plazmě. V *in vitro* studii byla použita lidská glioblastomová buněčná linie (U-87 MG) pro zjištění internalizace, saturace a kompetice připraveného [^{99m}Tc]Tc-MA peptidu.

Výsledky: Optimalizace radioaktivního značení dosáhla 100% radiochemické čistoty a [^{99m}Tc]Tc-MA peptid prokázal vysokou stabilitu v myší plazmě, s biologickým poločasem přesahujícím 180 minut. Navíc [^{99m}Tc]Tc-MA peptid prokázal dobrou internalizaci, kdy většina receptorem vázaného radioligandu byla internalizována po 90 minutách. Kromě toho byla pozorována i silná afinita [^{99m}Tc]Tc-MA peptidu k VEGFR2, s hodnotami rovnovážné disociační konstanty K_D = 103,2 nM a inhibiční koncentrace IC_{50} = 3,75 μM.

Závěry: Zjištěné výsledky naznačují, že by [^{99m}Tc]Tc-MA peptid mohl být považován za slibné radiofarmakum pro cílené zobrazování nádorů exprimujících VEGFR2 s potřebou dalších *in vivo* preklinických studií.

Klíčová slova: angiogeneze, peptid, technetium-99m, zobrazování tumorů, SPECT, VEGFR2

Content

1 INTRODUCTION

Angiogenesis, the process of forming new blood vessels from pre-existing ones, is a crucial physiological phenomenon that occurs throughout human life. This complex process is tightly regulated by various signaling pathways and is vital for numerous biological functions, including embryonic development, wound healing, and the formation of new blood vessels in response to increased tissue demands. Unlike vasculogenesis, which involves the *de novo* formation of blood vessels from mesodermal stem cells, angiogenesis builds on the existing vascular network. Angiogenesis involves several steps beginning with the degradation of the perivascular extracellular matrix by proteolytic enzymes. This degradation allows endothelial cells to migrate and form primary sprouts. These sprouts then proliferate, forming capillary loops that eventually mature into functional blood vessels. This process ensures adequate blood supply, delivering oxygen and nutrients necessary for tissue survival and function. The significance of angiogenesis extends beyond normal physiology; it is also implicated in pathological conditions, most notably in the growth and metastasis of tumours.

Tumours require a blood supply to obtain oxygen and nutrients, essential for their growth and metastasis. Tumour angiogenesis is often characterized by irregular and leaky vessels, differing significantly from normal physiological angiogenesis. The hypoxic environment within tumours triggers the release of angiogenic factors like Vascular Endothelial Growth Factor (VEGF), which stimulates the formation of new blood vessels, enabling tumour growth beyond a size of 1–2 mm^3. The VEGF/VEGF receptor (VEGFR) signaling pathway is particularly crucial in this process, making it one of the a key targets for cancer therapy.

Inhibiting angiogenesis can starve the tumour of its blood supply, thereby inhibiting its growth and potential to metastasize. Various antiangiogenic therapies have been developed, including monoclonal antibodies, tyrosine kinase inhibitors, and peptide inhibitors targeting the VEGF/VEGFR axis. These treatments aim to block the angiogenic signals, thereby preventing new blood vessel formation within tumours. Despite the initial success of antiangiogenic therapies, challenges such as drug resistance and limited efficacy in some patients remain. Tumours can develop alternative angiogenic pathways or increase the production of other pro-angiogenic factors, diminishing the effectiveness of VEGF/VEGFR inhibitors. Additionally, the systemic inhibition of angiogenesis can lead to side effects like impaired wound healing and vascular disorders. Hence, ongoing research is focused on developing more effective and targeted angiogenesis inhibitors with fewer side effects.

To overcome these challenges, research is focusing on the development of new therapeutic strategies, including the use of small peptide inhibitors and radiolabelled compounds for targeted therapy and diagnosis. In recent years, radiolabelled peptides have shown promise in both the diagnosis and treatment of angiogenic processes. These peptides can be used as tracers in molecular imaging to evaluate the efficacy of antiangiogenic therapies and to detect tumors with high angiogenic activity. Furthermore, they offer potential as therapeutic agents by delivering cytotoxic radionuclides directly to angiogenic tissues, thereby minimizing systemic toxicity.

Taken together, in the present study we aimed to develop and evaluate an 18-amino acid peptide (MA peptide) labelled with technetium-99m (^{99m}Tc) ([^{99m}Tc]Tc-MA) for targeting the VEGFR type 2 receptor.

2 THEORETICAL PART

2.1 Angiogenesis

Angiogenesis is a physiologic and complex process that is controlled by multiple signaling pathways to develop new blood vessels from the endothelium of the pre-existing vessels. The formation of a blood vessel system from an already existing one differentiates angiogenesis from vasculogenesis, which represents the formation of blood vessels *de novo*. Angiogenesis takes place at all stages of life, in both states of wellness and illness, starting during foetal development and persisting into old age (1). Capillaries are essential for the transportation and exchange of nutrients and metabolites in all tissues, therefore angiogenesis represents the important physiological process in tissue supply in time of its increased demand. Angiogenesis was first recorded by a Scottish anatomist and surgeon John Hunter who reported the enlargement of the vascular system during his surgery (2). Then, Judah Folkman described the modern history of angiogenesis and showed that tumour growth is an angiogenesis-dependent process (3). The cardiovascular system is the first organ system to form in the embryo. The inner surface of the circulatory system that comes into contact with blood consists of a single layer of endothelial cells derived from the mesoderm. Hemangioblasts, originating from mesodermal stem cells, differentiate into hematopoietic stem cells and angioblasts. Angioblasts cells then have the potential to differentiate into the endothelial cells (4). Overall, vasculogenesis includes the transformation of mesodermal stem cells into angioblasts, and the migration of angioblasts influenced by growth factors to form blood islands where they give rise to endothelial cells (5). In addition to occurring during foetal development *in utero*, angiogenesis can also take place in adults, a process referred to as sprouting angiogenesis.

At the first step of angiogenesis sprouting, proteolytic enzymes are secreted from surrounding stromal cells, including fibroblasts and inflammatory cells to degrade the perivascular extracellular matrix (ECM) and the basement membrane (BM) (6). These

proteolytic enzymes are classified into four main groups including cysteine-proteinase (e.g. Cathepsins), serine-proteinase (e.g. Elastase, Trypsin), aspartic-proteinase (e.g. Pepsinogen, Cathepsins), and metalloproteinases (e.g. Collagenase, Stromelysin) based on the type of amino acids in their active site (7, 8). Then, endothelial cells migrate into the perivascular area which forms primary sprouts. Then, the migrated endothelial cells start to proliferate in the primary sprouts, leading to the formation of capillary loops. Subsequently, maturation occurs which involves the synthesis of a new basement membrane and the formation of tube-like structures through which blood can flow (Figure 1) (9).

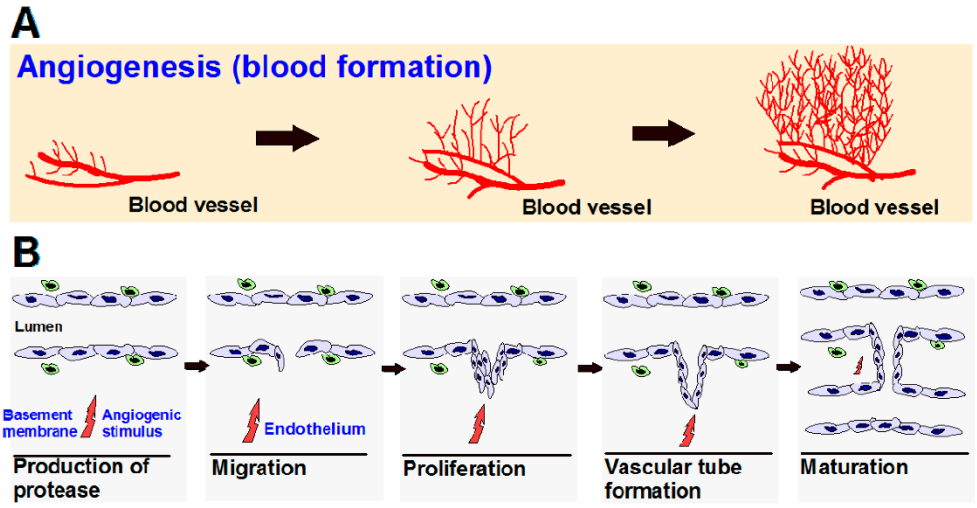

Figure 1 (A) Angiogenesis involves the growth of new blood vessels from existing ones, facilitating tumour advancement; (B) Stages in angiogenesis (10).

2.2 Angiogenesis process in tumour tissues

Natural angiogenesis processes play a vital role in embryo development, wound recovery, and the creation of collateral vessels for enhanced organ blood flow as in exercised mussels. However, angiogenesis has an important role in tumour growth, making it an ideal target for cancer therapy and diagnosis (11). For tumours either to grow or metastasize, they require oxygen and nutrients supplied by blood vessels. Without vascular support, tumours can become necrotic or undergo programmed cell death. The cancer cells without blood circulation grow to 1–2 mm^3 in diameter and then stop, but continue growing with the help of angiogenesis

(12). There is a significant difference between tumour angiogenesis and normal physiological angiogenesis (Figure 2).

Tumour angiogenesis initiates where the tissue's basement membrane is locally damaged mainly due to low oxygen levels. Vascular cells contain oxygen sensors that interact with the hypoxia-inducible transcription factor (HIF) family, which plays a crucial role in responding to oxygen fluctuations. The HIFα isoforms can interact with ARNT (aryl hydrocarbon receptor nuclear translocator also designated as HIF-1β) to activate the expression of numerous genes, including the vascular endothelial growth factor (VEGF) family and their receptors (VEGFRs) (13). Subsequently, endothelial cells, stimulated by the angiogenic factor VEGF, produce matrix metalloproteinases (MMPs) that break down the extracellular matrix, enabling the migration of endothelial cells (14). These cells then proliferate and stabilize, with angiogenic factors continuing to drive the process. Various angiogenic factor proteins have been identified as angiogenic activators including angiogenin, basic fibroblast growth factor (bFGF), epidermal growth factor (EGF), tumour necrosis factor alpha (TNF-α), transforming growth factor alpha (TGF-α) and beta (TGF-β), granulocyte colony-stimulating factor, platelet-derived endothelial growth factor, interleukin-8, and previously mentioned VEGF (12).

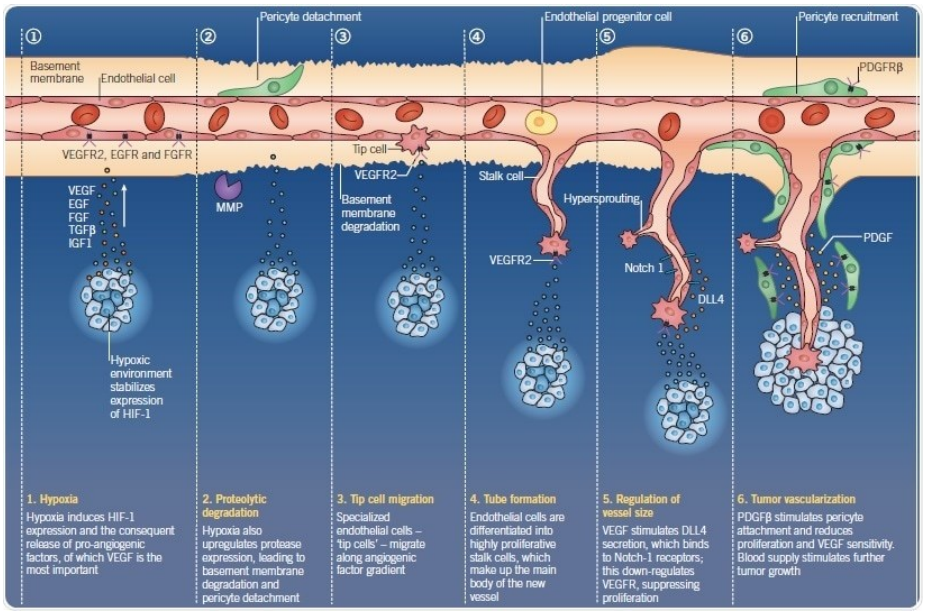

Figure 2 The process of angiogenesis in cancer tissue (15).

2.3 Targeting angiogenesis in cancer cells

Despite advances in therapeutic modalities including surgery, radiotherapy, and chemotherapy, treatment results are disappointing in patients who suffer from cancer. Therefore, a new therapeutic strategy is urgently required (16, 17). Due to the crucial role of angiogenesis in the process of tumour growth and metastasis, it became an ideal target for cancer therapy (18). The use of angiogenesis suppressors and receptor inhibitors can prohibit the neovascularization of cancer tissue as well as the growth of the tumour and thus might be beneficial to the treatment of cancer. Six classes of angiogenic inhibitors currently approved by the U.S. Food and Drug Administration (FDA) to be used for cancer therapy include monoclonal antibodies (e.g. Bevacizumab, Ramucirumab, Olaratumab), oligonucleotide derivatives (e.g. Pegaptanib), recombinant fusion proteins (Ziv-Aflibercept), mTOR inhibitor (e.g Everolimus, Temsirolimus), immunosuppressants (e.g Lenalidomide), and small molecule tyrosine kinase inhibitors (e.g. Sorafenib, Imatinib, Sunitinib) (19).

Nevertheless, there is universal agreement that vascular endothelial growth factor and its corresponding receptors particularly VEGF receptor type 2 (VEGFR2) play a central role in

angiogenesis. In addition, a high level of VEGF/VEGFR expression is also observed in human cancers including breast (20), colorectal (21), and Glioblastoma multiform (GBM) (22). Consequently, efforts in clinical settings have predominantly concentrated on the development of antiangiogenic therapies targeting the VEGF/VEGFR signalling pathway (23).

2.4 VEGF and VEGFR axis

Five VEGF ligands including VEGFA, VEGFB, VEGFC, VEGFD, and placenta growth factor (PlGF) have been recognized that could be expressed by different cell types and act in a paracrine and autocrine manner (24). Among these ligands, VEGFA (commonly called VEGF or VEGF-A) is the most extensively studied member of the VEGF family and exists in various isoforms including $VEGFA_{121}$, $VEGFA_{145}$, $VEGFA_{165}$, $VEGFA_{183}$, $VEGFA_{189}$, and $VEGFA_{206}$ created due to alternative splicing of mRNA during transcription of the human VEGFA gene. Each of these ligands has several variants due to or posttranslational modification and alternative splicing that binds to specific VEGFRs, and initiates different cell responses including inflammatory cell recruitment, fatty acid uptake, lymphangiogenesis, and angiogenesis (25).

Three types of VEGFRs including VEGFR1, VEGFR2, and VEGFR3 have been recognized that are structurally related to receptor tyrosine kinases (RTKs) (26). VEGFR1, also known as Fms-like tyrosine kinase 1, is not only expressed in vascular endothelial cells but also in other cell types including human trophoblasts, vascular smooth muscle cells, dendritic cells, monocytes, macrophages, and various types of cancer cells (27, 28). It has been reported that VEGFR1 could bind with VEGFA, initially identified as a vascular permeability factor (VPF), and is essential for vascular permeability, vasodilation, cell migration, mitogenesis, and endothelial cell sprouting (29). VEGFA also plays an important role in tumour growth, survival, metastasis, and migration through activating various signalling pathways including signal-regulated kinase 1/2, Src family kinases, and stress-activated protein kinase/c-Jun

NH_2-terminal kinase (30-33). In addition to VEGFA, PIGF also could bind to VEGFR1 which plays an important role in the regulation of inflammatory cell recruitment. It has been reported that PlGF also has an important role in tumour progression by promoting pathological angiogenesis (34, 35). VEGFB could bind to VEGFR1 and VEGFR2 inducing angiogenesis during embryonic development, and enhancing the coverage of perivascular cells, as well as facilitating metastasis, regardless of its impact through VEGFA (29).

As mentioned in the literature review, VEGFR2 expressed in both growing lymphatic and blood vessel systems, binds mainly to VEGFA and also proteolytically processed VEGFC and VEGFD, leading to physiological or pathological angiogenic responses in endothelial cells (36, 37). Extensive research also has shown that VEGFR1 is significantly upregulated in cancer tissues, resulting in the survival of cancer cells in prolonged low-oxygen conditions and could enhance a more aggressive cancer phenotype (38-40).

In contrast to the high expression of VEGFR2 in endothelial cells of vessels, studies have shown that VEGFR3 is mainly expressed in lymphatic endothelial cells. Previous research has established that the binding of VEGFC or VEGFD to VEGFR3, also known as Fms-like tyrosine kinase 4, is considered the main regulator of tumour and normal lymphangiogenesis (41). A study by Haiko et al. showed that deletion of VEGFC and VEGFD caused defects in lymphatic vessels (42). Moreover, there is a growing body of literature demonstrating that VEGFR3 enhances the formation of new lymphatic vessels from preexisting ones and could have an important role in increasing vascular density in several tumour types (43-45). Neuropilins-1 and -2 (NRP-1 and NRP-2) additionally function as co-receptors for VEGF ligands (46).

It has been demonstrated that the expression of VEGF is controlled by mechanisms that are both dependent on and independent of hypoxia. Under conditions of low oxygen, HIF1α

undergoes de-hydroxylation, preventing its degradation by the von Hippel–Lindau (VHL) protein, consequently leading to increased VEGF expression. Furthermore, aberrant activation of receptor tyrosine kinases in cancer cells can also induce hypoxia-independent upregulation of HIF1α and VEGF expression (47-50). After expression of VEGFR, they bind to their specific VEGFR on target cells, causing VEGFR auto-phosphorylation and activation of downstream signal transduction including the PI3K, PLC-γ, Akt, Ras, and MAPK pathways promoting proliferation, cell survival, migration, permeability, differentiation, modulation of cell-adhesion molecules (51-53).

2.5 Targeting VEGF/VEGFR in cancer therapy

2.5.1 Therapy targeting

As it has been shown in Figure 3, the VEGF/VEGFR axis plays a pivotal role in tumour angiogenesis by promoting endothelial cell sprouting, proliferation, and migration. It is secreted not only by cancer cells but also by stromal cells like endothelial cells and fibroblasts. VEGFR1 is predominantly found on myeloid cells, VEGFR2 on endothelial cells with sporadic expression on tumour cells, and VEGFR3 mainly on lymphatic endothelial cells (54). In addition to the key role of the VEGF/VEGFR axis in tumour angiogenesis, it has been revealed that this axis could promote the aggressive phenotype of cancer cells via induction of cancer cell stemness (55), epithelial-to-mesenchymal transition (EMT), tumour invasiveness (56), migration (57), and also chemotherapeutic resistance (58). Cancer cell stemness is induced via VEGF/NRP2-mediated activation of the Hippo pathway and VEGF/NRP1-mediated activation of the Wnt/β-catenin pathway (59, 60). VEGFA also could function as an immunosuppressive cytokine within the tumour microenvironment, hindering the activity of various immune cell types. More specifically, it interferes with the maturation and antigen presentation of dendritic cells, consequently suppressing T-cell-mediated cytotoxicity (54).

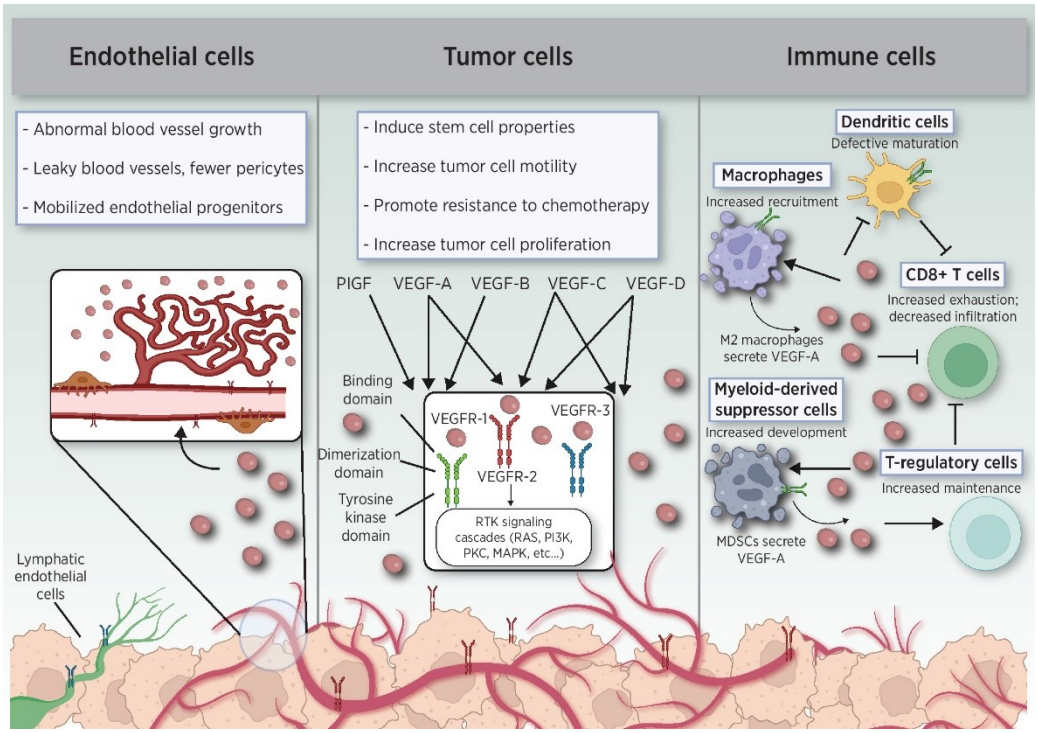

Figure 3 The impact of VEGF on the activity and proliferation of endothelial, tumour, and immune cells within the tumour microenvironment (54).

Therefore, inhibition of tumour angiogenesis via the targeting VEGF/VEGFRs pathway seems to be effective in the inhibition of tumour growth. Neutralizing antibodies to VEGF or VEGFRs, soluble VEGFR/VEGFR hybrids (Decoy receptor), and tyrosine kinase inhibitors of VEGFRs have been used as principal antiangiogenic molecules to target VEGFR/VEGFR axis (26). Since VEGFR2 is expressed in vascular endothelial cells and is the main receptor for angiogenic actions of VEGFA in cancer cells, inhibition of VEGFR2 binding to VEGFA has a great importance. VEGFR2 has a juxtamembrane domain (JMD), a split tyrosine kinase domain (TKD), an extracellular part with seven immunoglobulin-like domains (D1-7), a single transmembrane region (TMD), and a C-terminal tail (Figure 4).

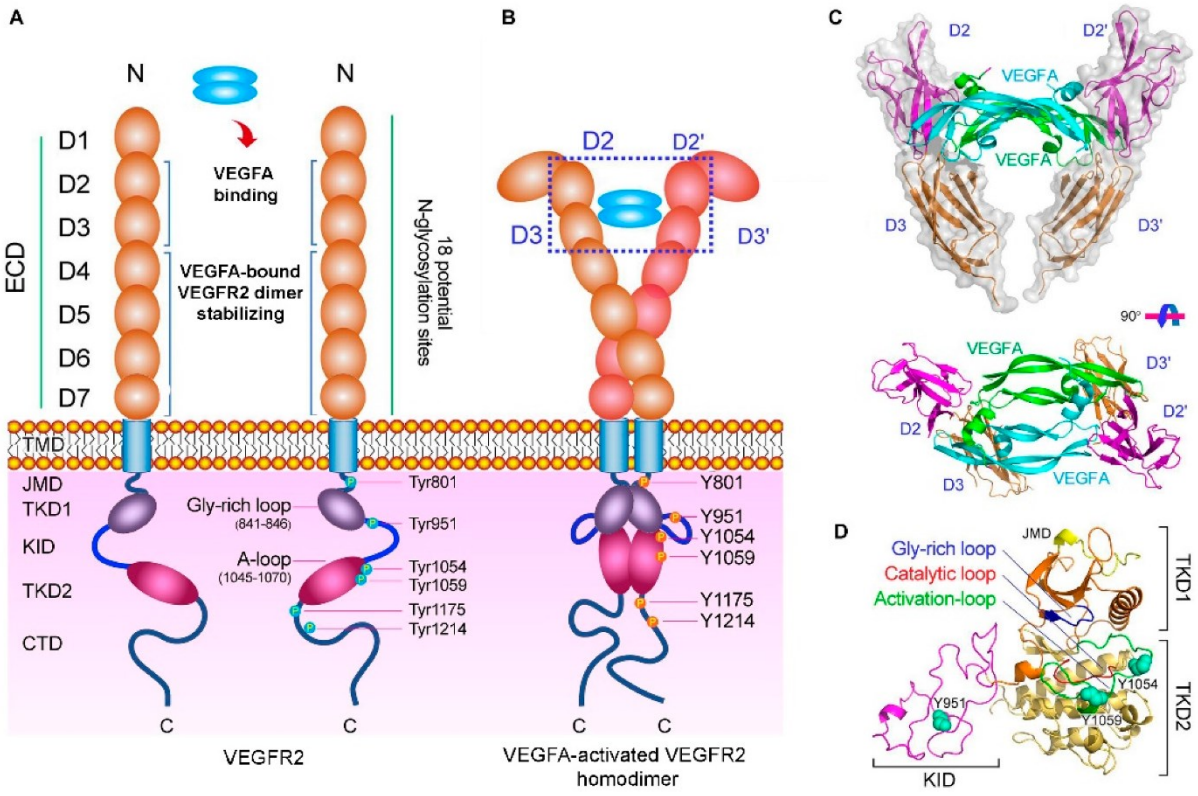

Figure 4 (A) Diagram of the VEGFR2 structure shows that it consists of an extracellular domain with seven Ig-like subdomains, a transmembrane domain, a juxtamembrane domain, a catalytic tyrosine kinase domain, and a flexible C-terminal domain. (B) When VEGFA binds to VEGFR2, it triggers the phosphorylation of various tyrosine residues in the tyrosine kinase domain. (C) The molecular structure of VEGFA binding to specific domains of VEGFR2 and (D) the structure of the tyrosine kinase domain is illustrated in the diagram (61, 62).

Upon activation, phosphorylated VEGFR2 subunits activate various adaptor molecules such as Shb, SOS, and Grb-2 that interact with and activate Ras GTPase, which in turn stimulates the MAPK pathway leading to endothelial cell proliferation. The phosphorylated intracellular VEGFR2 domain also activates PLC-γ, resulting in the hydrolysis of PIP2 to IP3 and DAG. IP3 triggers the release of Ca^{2+} from the endoplasmic reticulum, leading to the activation of various proteins including cAMP phosphodiesterase, adenylate cyclase, and eNOS, eventually promoting vasodilation and vascular permeability. In another way, DAG activates PKC, which promotes cell proliferation and migration. Additionally, phosphorylated VEGFR2 activates AKT, initiating the PI3K/AKT/mTOR pathway, which regulates the cell cycle, metabolism, and cellular functions (63, 64). VEGFR2 activation also leads to FAK

signalling involved in cellular migration, adhesion, cytoskeleton rearrangement, and tumour progression. VEGFA can also regulate endothelial cell attachment independently of VEGFR2 through NPR-1 (65) (Figure 5).

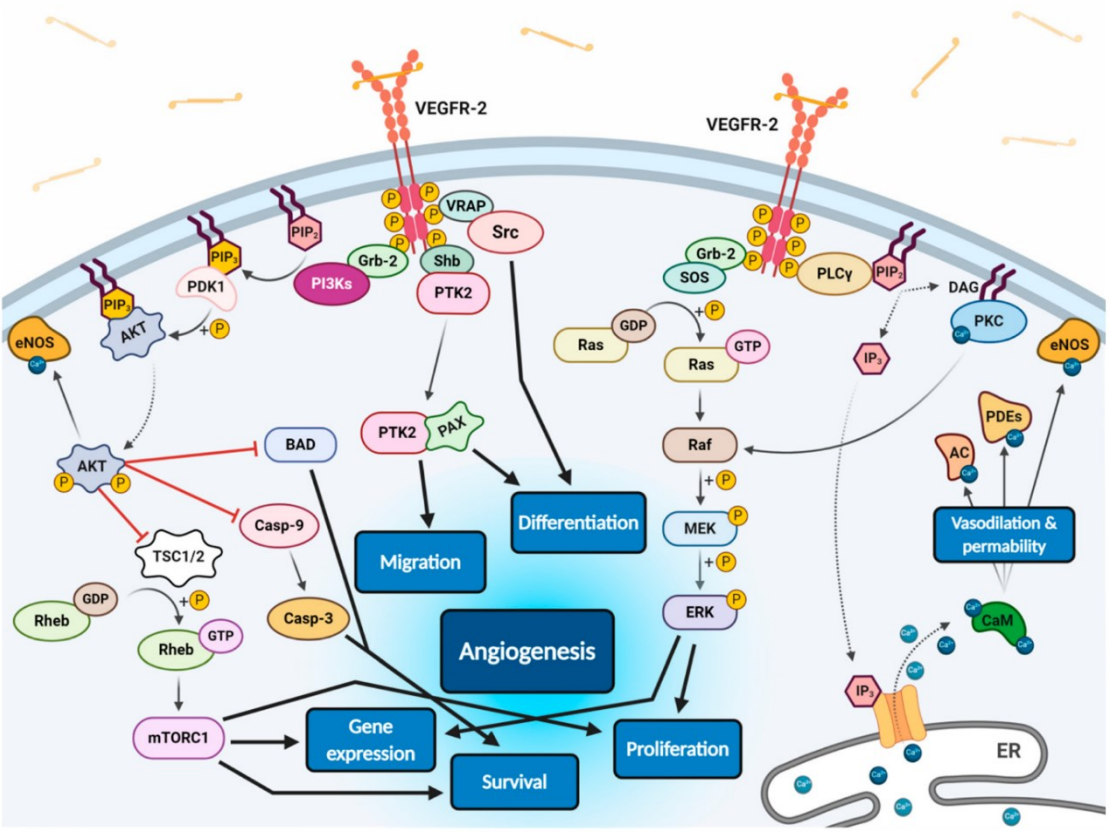

Figure 5 Diagram illustrating the signalling process of the VEGF-VEGFR2 ligand-receptor complex in endothelial cells (66).

Humanized monoclonal antibody Bevacizumab (Avastin®; Genentech Inc.) is the first antiangiogenic agent to be approved by the U.S. FDA, acting by inhibiting the VEGF activity (67). Bevacizumab has been used in combination with chemotherapy for the treatment of various cancers including nonsquamous cell lung carcinoma (NSCLC), metastatic renal cell carcinoma, and GBM (68-71). However, some other types of studies reported that the use of bevacizumab has been linked to a more aggressive and invasive tumour phenotype, especially in glioblastoma (72). Human monoclonal antibody Ramucirumab (IMC-1121B; Imclone

Systems) as the first introduced VEGFR2-targeting antibody also showed promising results in breast and gastric cancer (73).

Aflibercept, a fusion protein of VEGFR1 and VEGFR2, binds to VEGFA, VEGFB, and PlGF1 and 2, showing effectiveness in treating metastatic colorectal cancer (74). In addition to decoy receptors and neutralizing antibodies, small molecule inhibitors (SMIs) targeting VEGFR tyrosine kinase activity offer an important strategy for inhibiting VEGF-induced angiogenesis. Numerous tyrosine kinase inhibitors have been designed to specifically block VEGFR2, although they also affect other VEGFRs and tyrosine kinase receptors such as the EGFR family, Platelet-derived growth factor receptor alpha (PDGFR-α), and FGF receptor (26). Sunitinib and Sorafenib as multiple tyrosine kinase inhibitors and Pazopanib as pan-VEGFR inhibitors are some examples of SMIs that inhibit angiogenesis (75-77). Previous research has established that VEGF/VEGFR inhibition in combination with chemotherapy and immune checkpoint inhibitors could increase the efficacy of cytotoxic therapies and prevent tumour immune evasion, respectively (78). Current VEGF/VEGFR inhibitors that were approved firstly by the European Medicines Agency (EMA), National Medical Products Administration (NMPA), and U.S. FDA including those approved for use in combination with chemotherapy or anti-PD-1/PD-L1 therapy, have been listed in Table 1.

Table 1 Current VEGF/VEGFR therapy approvals (78-80).

Approved VEGF/VEGFR drugs	**First approval**	**Type**	**Target**	**Approved Indications**
Bevacizumab (Used in combination with atezolizumab, or chemotherapy)	2004 by FDA	mAb	VEGFA	GBM, NSCLC, CRC, BC, RCC, OC
Pegaptanib	2004 by FDA	Pegylated polynucleotide aptamer	$VEGF_{165}$	nAMD
Tivozanib	2017 by EMA	RTKI	VEGFR1/2/3	RCC

Approved VEGF/VEGFR drugs	First approval	Type	Target	Approved Indications
Ramucirumab	2014 by FDA	mAb	VEGFR2	CRC, NSCLC, GEJ, HCC
Aflibercept	2011 by FDA	Decoy receptor	VEGFA, VEGFB, PIGF	Metastatic CRC
Conbercept	2014 by NMPA	Recombinant fusion protein consisting of VEGFR-1 D2 and VEGFR-2 D3-D4	VEGF-A/B/C/D, PlGF	nAMD, DME
Apatinib	2014 by NMPA	RTKI	VEGFR2	Adenoid cystic carcinoma, gastric (approved by CDFA)
Anlotinib	2018 by NMPA	RTKI	VEGFR2/3 and PDGFRα/β, RET, FGFRs, c-Kit	NSCLC, STS, SCLC
Axitinib (Used in combination with Pembrolizumab and Avelumab)	2012 by FDA	RTKI	VEGFR-1/2/3, PDGFR	RCC
Cabozantinib (Used in combination with nivolumab)	2013 by FDA	RTKI	VEGFR2, MET, RET, AXL, Flt-3, c-Kit	HCC, RCC
Cediranib	2008 by EMA	RTKI	VEGFR1/2/3, PDGFR-a, CSF-1R, Flt3	Ovarian cancer, BRCA mt HER2– metastatic breast cancer
Levantinib (Used in combination with pembrolizumab)	2018 by FDA	RTKI	VEGFR2/3	Thyroid cancer, RCC, HCC, endometrial carcinoma
Nintedanib	2014 by FDA	RTKI	VEGF-1/2/3, PDGFR, FGFR1/3	idiopathic pulmonary fibrosis; NSCLC (EU approval)
Pazopanib	2009 by FDA	RTKI	VEGFR2	RCC, soft tissue sarcoma
Regorafenib	2012 by FDA	RTKI	VEGFR2/3, PDGFR-b, FGFR1/2, c-Kit, RET, B-Raf	CRC, HCC, GIST
Sorafenib	2005 by FDA	RTKI	VEGFR2/3, PDGFR-b, Flt-3, c-Kit, B-Raf	RCC, hepatocellular cancers, metastatic differentiated thyroid carcinoma

Approved VEGF/VEGFR drugs	First approval	Type	Target	Approved Indications
Sunitinib	2006 by FDA	RTKI	VEGFR1/2/3, PDGFR, Flt-3, RET	RCC, GIST, NE tumors of the pancreas
Vandetanib	2011 by FDA	RTKI	VEGFR2, EGFR, RET	MTC

Abbreviations: CRC, colorectal cancer; EU, European Union; GIST, gastrointestinal stromal tumours; HCC, hepatocellular carcinoma; MTC, medullary thyroid cancer; mt, mutant; NE, neuroendocrine; RCC, renal cell carcinoma; RTKI, receptor tyrosine kinase inhibitor; CDFA, China General Administration of Food and Drug Administration.

2.5.2 Challenges of VEGF/VEGFR targeted therapy: development of resistance and limited therapeutic response

Data from several studies suggest that despite the approval of different VEGF/VEGFR axis inhibitors, a significant number of patients fail to show even a transient clinical benefit. Intrinsic or acquired resistance to VEGF/VEGFR inhibition could be related to the redundancy of angiogenic factors (FGFs, PDGFs, PIGF) (81), high levels of infiltrating inflammatory cells that produce a number of proangiogenic factors (82), upregulation of alternative proangiogenic signals (83), increased production of proangiogenic factors by stromal cells (84), recruitment of bone marrow-derived proangiogenic cells (85), and increased vascular pericyte coverage (86). The hypoxic tumor microenvironment also could cause resistance to antiangiogenic therapies (87). Moreover, several significant toxicities have been observed in patients treated with antiangiogenic agents. It has been shown that the systemic application of anti-angiogenic compounds could lead to multiple side effects including impaired wound healing, vascular disorders in healthy organs, and in some cases caused ocular infections and retinal detachment (88, 89). Hence, the design of innovative VEGF inhibitors remains to be important.

The development of small peptide inhibitors targeting especially VEGFR2 shows great potential in creating innovative pharmaceuticals possessing the ability to bind to VEGFR2. For example, a study by Zhang et al. reported a novel peptide (HRHTKQRHTALH) that dose-dependently inhibits the proliferation of human umbilical vein endothelial cells stimulated by VEGF, *in vivo* and *in vitro* (90).

Peptides are usually stabilized by disulfide bonds, often contain less than 50 amino acids in length, and bind with high specificity to a protein of interest. Peptides serve as a valuable foundation in the creation of novel drugs that aim to interfere with interactions at protein-protein and protein-carbohydrate interfaces. This is due to the ease with which peptides can be synthesized, they are less toxic compared to SMIs and less immunogenic than antibodies (91). They don't accumulate in the body due to degradation by proteases and can be easily altered to align with the characteristics necessary for drug-like molecules and their half-life can be enhanced by the introduction of non-coded amino acids, cyclization, pegylation, acylation, or preparation of peptidomimetics (62).

2.6 Radiodiagnosis and radiotherapy of the angiogenic process

2.6.1 Therapeutical and diagnostic radionuclides

The search for potential biomarkers is important because they can help determine which patients are likely to benefit from certain treatments. Various biomarkers, such as VEGF levels, VEGFR expression, and imaging parameters, have been studied to predict sensitivity to antiangiogenic therapies (92). The level determination of VEGFA was one of the first biomarkers used for the assessment of cancer prognosis and also potential predictive analyte to identify response to VEGF/VEGFR signalling inhibitors (93). Identifying some single-nucleotide polymorphisms (SNPs) in VEGF genes was also reported to be important regarding anti-VEGF/VEGFR molecules (94). The evaluation of phosphorylated VEGFR2 level also has been considered essential in the prediction of the sensitivity to anti-VEGF/VEGFR molecules (95). In addition, several types of studies showed the importance and ability of radiolabelled VEGF ligands, radiolabelled anti-VEGF and anti-VEGFR antibodies, radiolabelled peptides, and radiolabelled SMIs for therapeutic and particularly diagnostic aims (66). These mentioned molecules are mainly labelled with radionuclides like lutetium-177 and rhenium-188 for therapy. Diagnostic radionuclides labelled compounds include in the case of single photon

emission tomography (SPECT) technetium-99m, indium-111, iodine-123, and iodine-125, and in the case of positron emission tomography (PET) fluorine-18, copper-61, copper-64, gallium-68 and zirconium-89 (96). Due to the advantages of targeting VEGF/VEGFR signalling using peptides as described before, the investigation of novel radiolabelled peptides seems to be valuable for cancer radiotherapy and radiodiagnosis.

2.6.2 Radiolabelled peptides for diagnosis and therapeutic purposes

Molecular imaging of tumour angiogenesis is reported to be important in the evaluation of response to anti-angiogenic therapies, determining whether to start and when to start anti-angiogenic therapies, patient stratification, development of novel drugs and personalized anti-cancer therapies, and lesion detection. Peptide-derived PET tracers offer benefits in terms of simplified synthesis and quality assurance (97). Some reports are proving that radiolabelled peptide-like structures could be used as radiotracers for VEGF/VEGFR system imaging. A study by Christoforidis et al. used ^{124}I-labelled Aflibercept, a recombinant fusion protein binding to both sides of the VEGF dimer to form an inert complex known as the VEGF trap, to assess its pharmacokinetic properties through sequential ocular imaging following intravitreal administration of the radioligand. Imaging studies in rabbit and owl monkey models also revealed that the radioligand mainly accumulated in the vitreous body with some presence in the thyroid gland (98). Another study by Hao et al., used [^{64}Cu]Cu-DOTA-GU40C4, a dimeric peptoid labelled with a positron emitter copper-64, as a highly potent antagonist of VEGFR2 for PET imaging of VEGFR2 expression in prostate cancer (PC3) xenograft mouse model. The acquired PET images showed that [^{64}Cu]Cu-DOTA-GU40C4 can be successfully used to image the expression of VEGFR2 (99).

Moreover, the potency, stability, and binding specificity of a cyclic nanopeptide RRL (Cys-Gly-Gly-Arg-Arg-Leu-Gly-Gly-Cys) with terminal intramolecular disulfide bridge toward VEGFR2 have been evaluated using ultrasonic imaging (MB-RRL) and optical method

(FITC-RRL or Alexa 680/800-RRL). A tyrosin was attached to RRL and was labelled with iodine-131. The results showed that [^{131}I]I-Tyr-RRL was stable in human serum and specifically accumulated in tumour, suggesting [^{131}I]I-Tyr-RRL as a potential compound for tumour radioimmunotherapy (100). Another study also reported the physicochemical and biological properties of ^{99m}Tc-labelled D(LPR) peptide. The study showed that ^{99m}Tc-labelled D(LPR) peptide had a high affinity to VEGFRs and high stability in saline and human serum, but unfortunately a low amount of tumour accumulation (101, 102).

In another *in vitro* and *in vivo* study by Barta et al. two ^{68}Ga-labelled peptides targeting VEGFRs were prepared as new PET tracers for tumour angiogenesis imaging in human glioblastoma and kidney carcinoma cells and the stability, *in vivo* biodistribution, and *in vitro,* affinity was evaluated. Both [^{68}Ga]Ga-NODAGA–peptides had an inhibitory concentration of 50% (IC_{50}) values in the range of 3.0–5.6 μM and an equilibrium dissociation constant (K_D) value in the range of 0.5–1.2 μM. A remarkable accumulation of both peptides was shown in the urinary bladder and the kidneys after intravenous application (103).

A recent study by Liu et al. also reported the efficacy of using an ^{89}Zr-labelled heterodimeric peptide for PET imaging of VEGFR and integrins in a U-87 MG cells murine glioma tumour xenograft model. The results showed that [^{89}Zr]Zr-DFO-heterodimeric peptide had a good binding ability to VEGFRs and integrins. Moreover, microPET/CT imaging after 1 to 3 h of [^{89}Zr]Zr-DFO-heterodimeric peptide injection visualized the U-87 MG xenograft cells. This study showed the potency of using radiolabelled peptide as a radiopharmaceutical compound for glioma tumours (104).

2.7 In-vitro drug experiments

In *in vitro* drug experiments with radiolabelled ligands including peptides, comprehensive characterization of the interaction between radiolabelled peptide and its

targeted protein-like receptor is crucial. This involves determining the internalization rate, saturation levels (K_D values), and competitive binding (IC_{50} values). These parameters provide a detailed picture of how a radiolabelled peptide interacts with its target, offering insights into its potential as a therapeutic or diagnostic agent.

2.7.1 Internalization study

The process of internalization is fundamental to the biological efficacy and mechanism of action of receptor-targeted radiolabelled ligands including peptides and facilitates drug development. Actually, internalization refers to the cellular uptake of receptor-ligand complexes, which can initiate signalling cascades, or be targeted for intracellular degradation (105). Intracellular degradation could occur as a result of internalization and represent an alternative route of elimination in addition to hepatic, reticuloendothelial, and renal clearance pathways that affect drug exposure and ultimately efficacy (106). The effectiveness of certain medications, like immunotoxins and antibody-drug conjugates, relies on how well they are taken up by their target cells to deliver the medication. Therefore, internalization can affect the efficacy of compounds and assessment of internalization kinetics is important during development and research (107).

There are different ways to evaluate internalization including qualitative and quantitative determination. Most of the articles used qualitative approaches such as using cleavable biotin (108, 109) or using flow cytometry (110, 111). It has also been reported that some quantitative internalization methods such as toxin-killing assays or acid dissociation measure the amount of internalization indirectly. The toxin-killing method assesses internalization by observing the cell-killing activity of antibody-toxins that have been internalized. On the other hand, the acid dissociation method evaluates the internalization of antibodies by measuring the quantity of internalized molecules after removing surface molecules using acid (112, 113). Another method that is extensively used for evaluating

internalization is the fluorescence-based imaging method. In this method, fluorescence microscopy has been used to visualize the fluorescent signal produced as a result of the internalization of a fluorescence-labelled ligand like antibody or receptor (114, 115).

For receptor-targeting peptides, understanding the rate and extent of internalization is essential as it impacts both the pharmacokinetics and therapeutic efficacy of the peptide. The internalization rate (K_{int}) can be determined by tracking the uptake of radiolabelled peptides into cells expressing targeted receptors over time. This approach uses techniques such as gamma counting in both supernatant (surface-/receptor-bound peptide fraction) and cell pellet (internalized radioactive peptide fraction) to quantify total receptor binding and internalized radioactivity using cell-associated activity during different times (116). Internalization curves are generated by plotting the percentage of total internalized radioactivity in the cells or supernatant (surface-bound peptide) versus time.

2.7.2 Efflux study

The release of internalized radioligand from cells could be measured by the efflux study. In this method, the amount and rate of radioligand release from within the cells are assessed over time, and cellular retention of the radioligand is calculated. When radioligand is rapidly released from cells, it indicates that there is likely not much retention in the target tissue. On the other hand, if there is a slow release of only a small amount of radioligand from cells, it could mean that a significant amount of the radioligand is retained in the target tissue for an extended period.

To measure the efflux of radioligand, radioligand is first added to cultured cells. Once radioligand is taken up by cells, a cell medium is removed, cells are washed with PBS, and a fresh medium is added. Radioligand released from cells into the medium is then quantified at different time points. Additionally, the amount of radioligand that has been internalized by

cells is determined in the total cell lysate. Finally, the efflux curve is generated by plotting the percent of initially internalized radioligand released over time from cells versus time (117).

2.7.3 Saturation kinetics and equilibrium dissociation constant (K_D)

Saturation binding is a technique used to evaluate the extent of specific receptor-mediated uptake of a radiolabelled ligand by measuring the increase in radioligand concentration. It means that saturation describes how radiolabelled ligand for example peptide concentration affects receptor binding at equilibrium. The equilibrium dissociation constant (K_D) is a critical parameter that indicates the affinity of a radiolabelled ligand to its receptor. To measure K_D, the amount of radioligand needed for saturation of receptor is determined and defined as the concentration of radioligand at which half of the available receptors are occupied under equilibrium conditions. This value is determined through binding assays where different concentrations of radiolabelled ligands are incubated with a constant amount of target cells. Culture medium is removed after the incubation period and cells are washed to determine the radioactivity value. Finally, by analysing the binding data, nonlinear regression of the saturation curve data yields the K_D value. The saturation diagram is generated by plotting the specific binding versus radioligand concentration. In fact, K_D is the ratio of the dissociation rate constant (k_{off}) to the association rate constant (k_{on}). Finally, a lower K_D value indicates a higher affinity, which is often associated with increased biological activity and potential therapeutic efficacy (118).

2.7.4 Competition assays and the determination of IC_{50} values

Competition assays are used to evaluate the competitive binding efficacy of a test compound against a known ligand for binding to its protein like receptor. Actually, these assays are used to determine the concentration of ligand of interest (for example a radiolabelled peptide) needed to reduce the specific binding of a standard. The pivotal condition is the binding of the tested ligand and standard to the same targeted structure site. Via analysing the

data, the inhibitory concentration at 50 % (IC_{50}) value, which is the concentration of a competitor required to inhibit 50 % of the specific binding of the standard is determined. The lower IC_{50} value shows higher receptor binding affinity because a lower concentration of a ligand of interest is needed to compete with a standard ligand. Therefore, IC_{50} is a key measure of the potency of a competitor and is used to rank and compare the different ligands' binding affinity toward targeted structures.

The determination of IC_{50} values might include the following arrangement. A fixed concentration of a radiolabelled standard (a compound with determined binding ability) is incubated with cells in the presence of increasing concentrations of a non-radioactive ligand of interest. After incubation, medium is removed, cells are washed and the amount of a radiolabelled standard bound to the membrane is determined. The IC_{50} is calculated from the dose-response curve obtained by plotting the membrane-bound radioactivity against the logarithm of a competitor concentration and data are analyzed using non-linear regression (118). The experiment conduction can be in the opposite order when a standard is non-radioactive with increasing concentrations competing with radiolabelled ligand of a fixed concentration.

3 ASSIGNMENT – AIM OF THE WORK

The aim of the presented study was focused on:

a) the radiolabelling of MA peptide with technetium-99m
b) the radiochemical purity assessment performed with HPLC analysis with radiometric detection
c) the stability testing of prepared [^{99m}Tc]Tc-MA peptide in mouse serum
d) the cell culturing of human glioblastoma cell line (U-87 MG)
e) the performance of *in vitro* binding experiments with [^{99m}Tc]Tc-MA in cell line comprehending internalization, saturation, and competition study
f) the acquired data processing and evaluation in MS Office Excel and GraphPad Prism programs
g) the comparison of obtained data with previously published scientific works in discussion chapter

4 EXPERIMENTAL PART

4.1 Device and Software employed

A shaker Vortex V1 plus (Biosan)

Analytical balances (Sartorius analytic)

Automatic pipettes (in pipetting scale 0,5-10 µL, 2-20 µL, 20-200 µL, 100-1000 µL;

Eppendorf Research Plus)

Bürker´s cell counting chamber (Brand)

Cell culture incubator (Sartorius Stedim Biotech product Certomat® CS-18)

Centrifuge U-32 R (Boeco)

Chemical extractor fan (Polon)

Dry-bath (MS Science)

Gamma Counter (Automatic Gamma Counter, Waltec Wizard2 3´´, 2480 Perking

Elmer)

HPLC system (Agilent 1100 Series, Agilent Technologies Inc.) with radiometric detection

Laminar flow box (Bio Air Instruments)

Magnetic stirrer (IKA RTC basic)

Microcentrifuge (Sprout, Heathrow Scientific)

Microscope (XDS-IR, OPTICA)

Multipette E3 (the pipetting scale up to 50 mL; Eppendorf Research Plus)

Multichannel pipette (Comfort)

Non-sterile cell culture incubator (Sanyo Incubator MIR-153)

pH meter (Eutech Instruments pH510)

Preliminary weights (Kern PLB 200-3)

Program GraphPad Prism (version 10.1.2)

Program Excel (Microsoft Office 365)

Spectrophotometer (TECAN INFINITE M200 PRO)

Surface radiation contamination detector (Polon)

Water bath TW12 (Julabo)

4.2 Material used

24-well cell culture plate (TPP)

96-well cell culture plate (TPP)

Cell culture flask (75 cm^2, TPP)

Gas burner (Schuett Phoenix)

Glass Pasteur´s pipette (Brand)

HPLC vials (Agilent Technologies)

LC column (ZORBAX Eclipse XDB-C18. 4.6x150 mm, 5 µm, Agilent Technologies)

Pipette tips (of volume 10 µL, 200µL, 1000 µL, Eppendorf)

Sterile serological pipettes (of volume 5, 10, or 25 mL, TPP)

Vial inserts (of volume 250 µL, Agilent Technologies)

Volumetric flask (volume 250 mL and 1 L, Simax)

4.3 Chemical used

70% ethanol (Penta)

37% HCl (Sigma-Aldrich)

Acetonitrile (HPLC quality, Honeywell)

$CaCl_2$ (Penta)

Calcium α-D-heptagluconate hydrate (Sigma-Aldrich)

cell culture medium (Dulbecco´s Modified Eagle´s Medium - high glucose (DMEM), Sigma-Aldrich)

Cu^{2+} ions (Merck)

Dimethylsulfoxid (DMSO, Merck)

Distilled water (Millipore)

Ethylenediaminetetraacetic acid (EDTA, Merck)

Fetal bovine serum (Merck)

Glucose (Penta)

Glycine (Merck)

HCl (Penta)

HEPES (Thermo Fisher Scientific)

KCl (Penta)

L-glutamine cell culture sterile solution (Sigma-Aldrich)

nitrogen (inert gas, Linde Gas)

MA peptide (custom synthesized 18 amino acids peptide, Apigenex)

$MgCl_2$ (Penta)

NaCl (Penta)

$Na_2HPO_4.12H_2O$ (Penta)

$NaH_2PO_4.2H_2O$ (Penta)

NaOH (Penta)

Non-essential amino acids solution (sterile, cell culture, Sigma-Aldrich)

Penicillin-Streptomycin solution for cell culture (Sigma-Aldrich)

Pierce BCA Protein Assay Reagent A (Thermo Scientific)

Pierce BCA Protein Assay Reagent B (Thermo Scientific)

Pyruvate solution (sterile, for cell culture, Sigma-Aldrich)

$SnCl_2.2H_2O$ (Penta)

Technetium-99m solution ($[^{99m}Tc]TcO_4^-$ in saline solution, GE Halthcare)

Trifluoracetic acid (Sigma-Aldrich)

Tris(hydroxymethyl)aminomethane (Merck)

Triton X (Sigma-Aldrich)

Trypsin-EDTA solution (sterile, Sigma-Aldrich)

4.4 Used biological material

The human glioblastoma cell line (U-87 MG, under the code HTB-14) (Figure 6) was acquired from the American Type Culture Collection (ATCC).

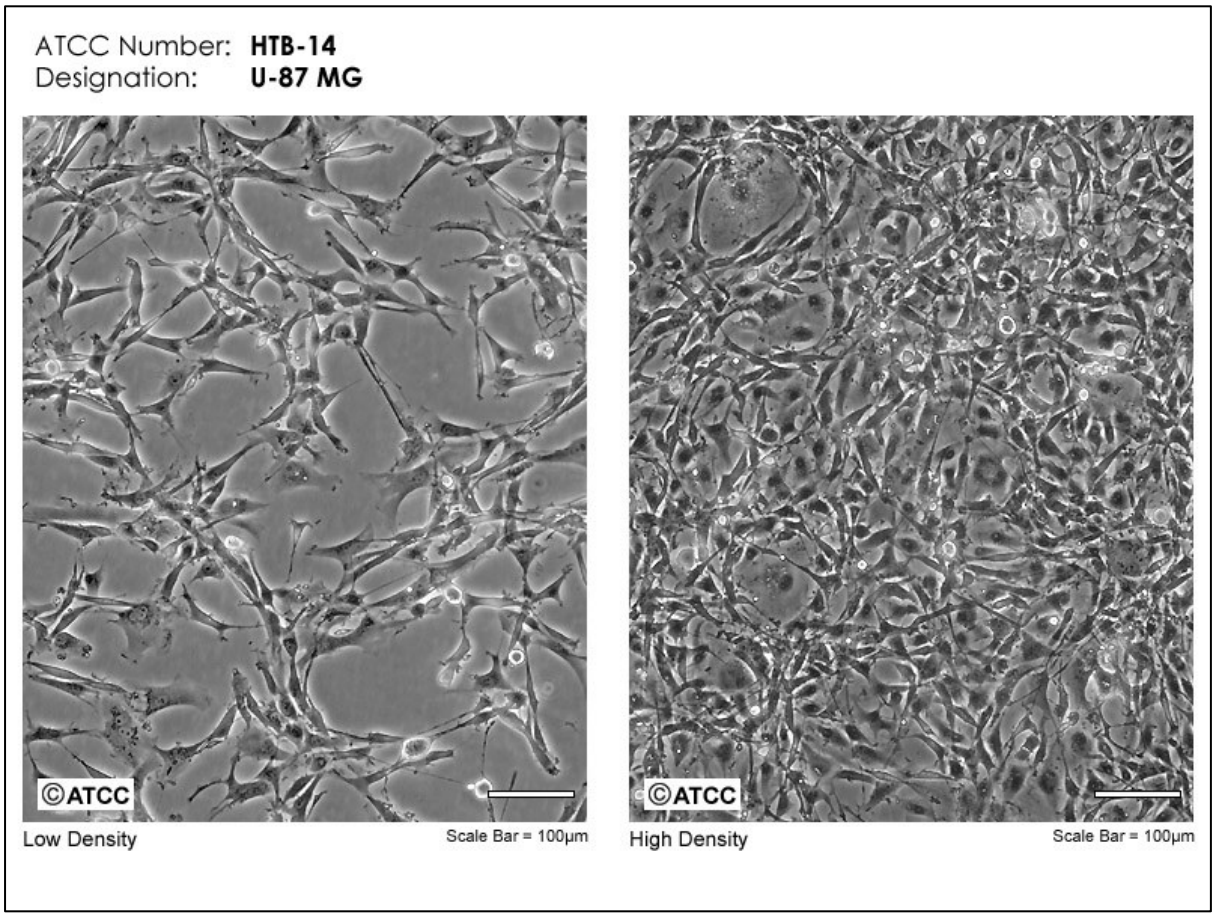

Figure 6 The morphology of low and high-density growth of human glioblastoma cell line U-87 MG (HGT-14) (Reference: https://www.atcc.org/products/htb-14)

4.5 Workflow

4.5.1 MA peptide synthesis

The 18 amino acid peptide was custom synthesized according to a previously published structure (acetyl-KLTWMELYQLAYKGI-amide) with a small modification (117). The ^{99m}Tc-binding moiety consisting of three more amino acids (lysine, aspartic acid, and cysteine)

was added to the N-terminus (Figure 7). The final molecule acetyl-KLTWMELYQLAYKGIKDC-OH further referred to as MA peptide (MW = 2245.7 g/mol) was analysed by UPLC MS (Waters Acquity TUV Detector, Waters Corporation, MA, USA) performed by the producer with the found product chemical purity over 96.1 % (Figure 8).

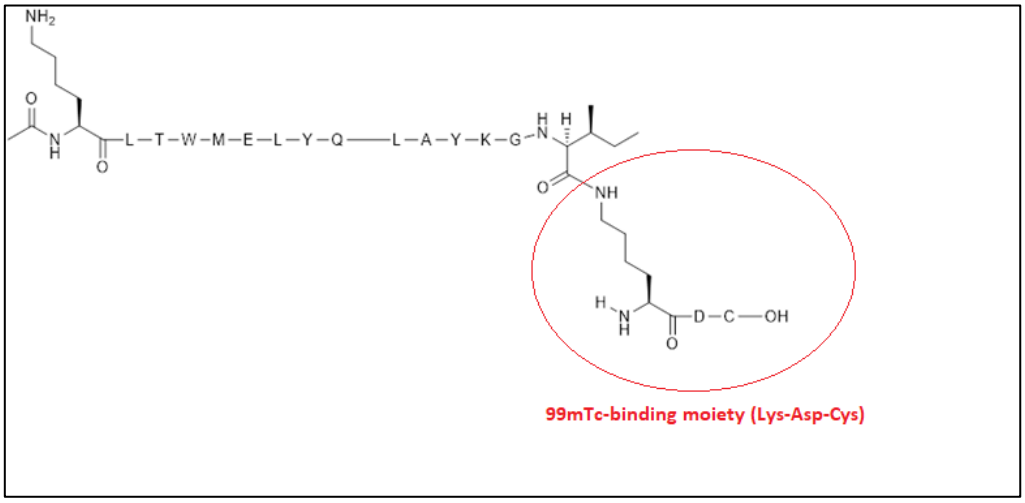

Figure 7 The chemical structure of MA peptide with ^{99m}Tc-binding moiety of amino acids lysine, aspartic acid and cysteine respectively in red circle.

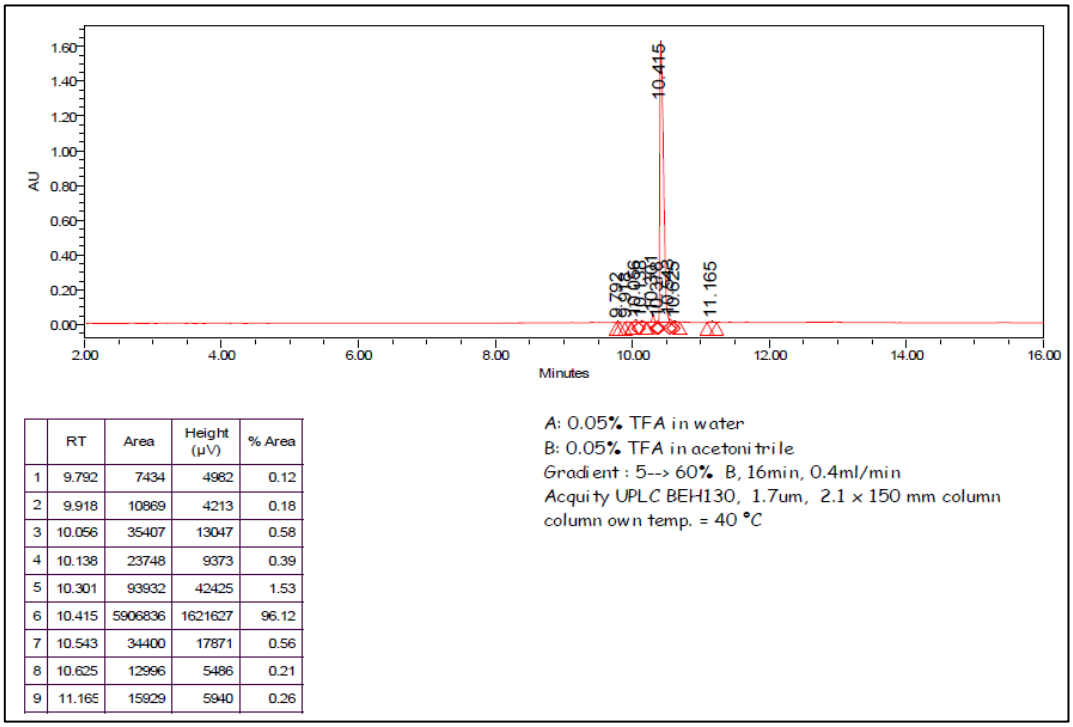

	RT	Area	Height (μV)	% Area
1	9.792	7434	4982	0.12
2	9.918	10869	4213	0.18
3	10.056	35407	13047	0.58
4	10.138	23748	9373	0.39
5	10.301	93932	42425	1.53
6	10.415	5906836	1621627	96.12
7	10.543	34400	17871	0.56
8	10.625	12996	5486	0.21
9	11.165	15929	5940	0.26

Figure 8 Chromatogram of MA peptide analysis after its synthetization with the elution peak at 10.4 min of UPLC run with the area under curve of the value 96.1 %.

4.5.2 ^{99m}Tc-labelled MA peptide preparation

The radiolabelling of MA peptide was performed according to a modified previously published protocol (Cazzamalli et al., 2016). MA peptide (5.8 nmol) in PBS (50 µL, pH 7.4) was added into a solution (150 µL) of calcium glucoheptonate (20 mg, Merck) with $SnCl_2$ (300 µg, Merck). Tris-buffered saline (600 µL, pH 6.69) was added and the final mixture was degassed for 5 min with nitrogen gas. The addition of [^{99m}Tc]TcO_4^- (0.8 MBq, ±1.2 µL, GE Healthcare) into the MA peptide mixture followed and the radiolabelling reaction proceeded for 20 min at 90 °C. The prepared radioligand [^{99m}Tc]Tc-MA peptide was analysed on radiochemical purity after the radiolabelling.

4.5.3 ^{99m}Tc-labelled MA peptide radiochemical purity control

[^{99m}Tc]Tc-MA peptide was checked on radiochemical purity with the employment of high-performance liquid chromatography (HPLC). Distilled water (0.1 % TFA) and acetonitrile (0.1 % TFA) as components of the mobile phase (flow rate 1.0 ml/min, gradient elution 0 to 80 % water/acetonitile in 20-min run) and the ZORBAX Eclipse XDB C18 4.6 × 150 mm column were used for the separation with HPLC equipped with a radiometric detection. The analysis of ^{99m}Tc-labelled MA peptide radiochemical purity always proceeded after the performed radiolabelling.

4.5.4 Cell culturing

U-87 MG cells were maintained and cultured in DMEM (high glucose) supplemented with penicillin (100 U/mL), streptomycin (100 mg/mL), non-essential amino acids (1 %), pyruvate (1 %) and FBS (10 %) at 37°C in a humidified atmosphere with CO_2 (5 %). The cells were cultured, stored, and passaged following ATCC guidelines.

U-87 MG cells are isolated from human glioblastoma and express the target VEGFR2 on their cell surface. The cells were cultured in culture bottles with the area of 75 cm^2. The work with cells proceeded under sterile conditions in the laminar box. All tools needed for cell culturing work have been sterilized with 70% ethanol before being placed in the laminar box

to maintain a sterile environment. Cells were cultured until became confluent and they underwent trypsinization and seeding in a new culture flask.

When needed for *in vitro* experiments, cells were seeded in the 24-well plate 48 hours before an experiment, when $1x10^5$ cells were transferred in each well. The exact number of cells after their release by trypsin was determined using Bürker's counting chamber. Cells deployed in this way were cultured under conditions identical to conventional cell line cultivation.

4.5.5 Phosphate buffer preparation

Phosphate buffer (PBS) maintains a pH of about 7.4 and was used for a cell wash and as a solvent for lyophilized MA peptide when radiolabelled. To prepare 1 litre of PBS buffer solution, NaCl (8.01 g), KCl (0.21 g), Na_2HPO_4 (3.58 g), and NaH_2PO_4 (1.56 g) were weighed. The weighed raw compounds were dissolved in distilled water and dissolved in a volumetric flask, which was then topped up with distilled water reaching a volume of 1 L. Subsequently, the pH value of the buffer solution was adjusted to 7.4 using NaOH (1 M) or HCl (1 M). PBS solution was kept in a refrigerator to avoid bacterial degradation.

4.5.6 Glycine buffer preparation

Glycine buffer was used for *in vitro* binding studies comprehending the internalization study. Glycine buffer causes the release of a non-internalized receptor-ligand complex from a cell surface. For the preparation of 200 mL of glycine buffer of the concentration 0.2 M with pH 2.8, 3 g of glycine was dissolved in 0.2 L of distilled water, and HCl (1 M) was used to adjust the pH value.

4.5.7 Krebs-Ringer´s solution preparation

Krebs-Ringer´s solution was used in *in vitro* binding studies comprehending the internalization, saturation, and competitive study. It serves as a medium added to cells with a tested radiolabelled compound. Its advantage lies in isotonic character, it is the source of energy for cells and is free of potential competing molecules. One litre of Krebs-Ringer´s solution was

prepared from NaCl (7.2 g), KCl (0.40 g), $CaCl_2$ (0.13 g), $MgCl_2$ (0.16 g), Na_2HPO_4 (0.29 g), NaH_2PO_4 (0.03 g), glucose (0.99 g) and HEPES (2.38 g). The weighed compounds were dissolved in distilled water. Subsequently, the pH value of Krebs-Ringer´s solution was adjusted to 7.4 using either NaOH (1 M) or HCl (1 M).

4.5.8 Disintegration solution preparation

The disintegration solution was prepared to lyse cells at the end of *in vitro* studies, thus producing cell lysate used to assess the cell protein content. The preparation of the disintegration solution of the volume 200 mL comprehended the weighing of 0.8 g of NaOH, its dissolvement in distilled water, and the final addition of Triton X (1 mL).

4.5.9 BCA Protein Assay

This commercial method is used, among others, for the assessment of cellular protein content. The assay is based on bicinchoninic acid (BCA) colourful complex formation with reduced copper ion (Cu^{1+}), which is reduced from oxidation state 2^+ by peptide bonds present in a sample.

Duplicates of cell lysate samples (20 µL) were taken from each well of the 24-well plate used in the *in vitro* experiment and placed in the 96-well plate. The amount of cell protein was determined from the linear dependence equation of the calibration series, which was prepared using bovine serum as a standard with a concentration in the range of 0-2000 µg/mL. 200 µL of BCA Protein Assay Mixed Reagent Solution was added to each lysate sample. The incubation followed at 37°C for 30 min. When incubation was over, the intensities of colour complex were measured in a spectrophotometer at a wavelength of 590 nm. The amount of cellular protein was calculated according to the calibration curve in MS Office 365 Excel. When data of measured activity (CPM) were obtained, they were calculated per cell protein concentration.

4.5.10 In vitro stability of [^{99m}Tc]Tc-MA peptide procedure

The radiolabelled peptide was tested on its stability in mouse serum at 37 °C in the time intervals 0, 30, 60, 90, 120, 140, 160 and 180 min after radiolabelling.

The prepared sample of ^{99m}Tc-labelled MA peptide was added into serum in the ratio 1:4, and incubated at 37 °C. At the above specified time points, stability aliquots (100 µL) were analysed in HPLC with radiometric detection as described above for the radiochemical purity analysis.

4.5.11 The *in vitro* internalization study with ^{99m}Tc-labelled MA peptide

Cellular internalization of VEGFR2-targeting [^{99m}Tc]Tc-MA peptide was analysed in U-87 MG cells at 37°C, at which all metabolic processes including receptor internalization are active.

First, 5×10^5 of U-87 MG cells were seeded in a 24-well plate. After 48-h incubation, cells were washed twice with PBS (0.7 mL) and then incubated with Krebs-Ringer´s solution (0.5 mL) containing [^{99m}Tc]Tc-MA peptide (90 nM) for the following time points: 15, 30, 45, 60, 75 and 90 min. Each time point was made in triplicates. Non-specific binding was analysed simultaneously in the same experimental setting varying in addition of natural MA peptide (1 μM) into each well.

When the incubation was over, cells were washed twice with ice-cold PBS (0.7 mL) and incubated with ice-cold glycine buffer (0.5 mL) for 1 min. Glycine wash was collected into centrifugal microtubes and cells were further lysed in disintegration buffer (0.5 mL). Lysate was collected into centrifugal microtubes, from which a sample of cell lysate (2 x 20 μL) was pipetted into a 96-well plate for cell protein analysis. Next, the gamma counter was used to measure the radioactivity in both glycine buffer wash (representing receptor-bound activity) and cell lysate (representing internalized activity). The combined radioactivity, including surface-bound and internalized counts (CPM) corrected on CPM measured in non-specific binding set, was plotted against the time points in the GraphPad Prism program. Each time point was made in triplicate of wells and each experiment was made in three independent repetitions.

4.5.12 The in vitro saturation study with ^{99m}Tc-labelled MA peptide

The binding affinity of ^{99m}Tc-labelled MA peptide to VEGFR2 was assessed through a saturation binding assay. First, 5×10^5 of U-87 MG cells were seeded in a 24-well

plate. After 48 h incubation, cells were twice washed with PBS (0.7 mL). The addition of Krebs-Ringer´s solution (0.5 mL) containing [^{99m}Tc]Tc-MA peptide with increasing concentrations (0, 9, 90, 180, 360, 720, and 1440 nM) followed. Non-specific binding was made in the same experimental setting with extra addition of natural MA peptide (1 uM). The incubation proceeded at 37°C for 90 min.

After the incubation, cells were twice washed with ice-cold PBS (0.7 mL) and lysed in a disintegration solution (0.5 mL). Subsequently, cell lysate was pipetted into centrifugal microtubes, when a sample of cell lysate (2 x 20 µL) was transferred into a 96-well plate for cell protein analysis. Cell lysate in centrifugal microtubes was measured in a gamma counter, and the binding data were analysed using MS Office Excel and GraphPad Software Prism, in which the final activity values (CPM) corrected on non-specific binding were plotted against concentration values (nM). As a result, the equilibrium dissociation constant (K_D), which reflects radioligand binding activity, was determined. Each concentration value was made in triplicate of wells and each experiment was made in three independent repetitions.

4.5.13 The *in vitro* competition study with ^{99m}Tc-labelled MA peptide

To determine the concentration of ligand inhibiting 50 % of maximum specific binding (IC_{50}) of a competitor, competition experiments were conducted using ^{99m}Tc-labelled MA peptide and its non-radiolabelled counterpart. First, $5x10^5$ U-87 MG cells were seeded in a 24-well plate. After 48-h incubation, cells were washed twice with PBS (0.7 mL) and the addition of Krebs-Ringer´s solution (0.5 mL) with [^{99m}Tc]Tc-MA peptide (90 nM) followed together with non-radiolabelled MA peptide at varying concentrations (0.1, 1, 10, 100, 1000 and 10000 nM). The incubation proceeded at 37°C for 90 min.

After the incubation, each well with cells was twice washed with ice-cold PBS (0.7 mL) and the addition of disintegration solution (0.5) followed. Cell lysate was pipetted into centrifugal microtubes when a lysate sample (2 x 20 μL) for cell protein assessment was taken into a 96-well plate. Radioactivity (in CPM) in each centrifugal microtube was measured in gamma counter and obtained data were processed in MS Office Excel and GraphPad Prism. As a result, the inhibitory curve was obtained to characterize the inhibitory concentration of radioligand. Each concentration value of the competitor was made in triplicate of wells and each experiment was made in three independent repetitions.

5 RESULTS

5.1 The radiolabelling and radiochemical purity analysis

The radiolabelling of MA peptide with technetium-99m was optimized in the ratio of activity added to MA peptide molecular mass so as to achieve 100% radiochemical purity, which was proved by HPLC analysis. The example overlay of radiochromatograms for free technetium-99m and [^{99m}Tc]Tc-MA peptide is demonstrated in Figure 9. Free technetium-99m had a retention time of 2.5 min and [^{99m}Tc]Tc-MA peptide was eluted at 12.5 min. No other peaks were detected in radiochromatograms. The result proved an excellent radiochemical purity based on the presence of a single radioactivity peak corresponding to ^{99m}Tc-labelled MA peptide, which allowed the further application of radioligand in *in vitro* experiments.

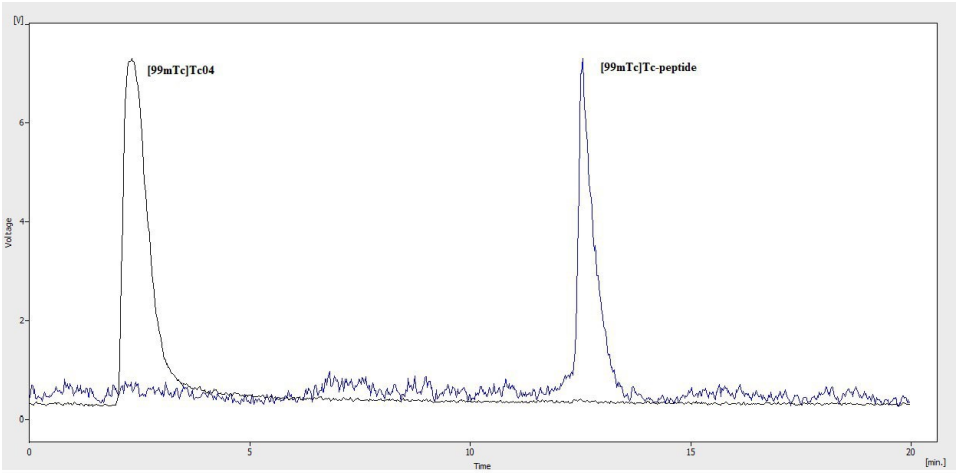

Figure 9 The demonstrative overlay of radiochromatogram of *technetium-99m free form (retention time 2.5 min) and ^{99m}Tc-labelled MA peptide (retention time 12.5 min) analysed by* HPLC *with radiometric detection.*

5.2 Stability determination

The results of the stability assessment presented in Table 2 showed that 73.9 % of ^{99m}Tc-labelled MA remained in the mouse serum after 180 min, verifying that the half-life of [^{99m}Tc]Tc-MA peptide is more than 180 min.

Table 2 Stability of prepared sample of 99mTc labelled MA peptide tested in mouse serum at 37 °C in the indicated time intervals after radiolabelling

Time (min)	[^{99m}Tc]Tc-MA peptide (%)	Free technecium-99m (TcO_4^-) (%)
0	100	0.0
20	100	0.0
40	100	0.0
60	100	0.0
80	100	0.0
100	85.5	14.3
120	90.2	9.8
140	69.9	30.1
160	82.4	17.6
180	73.9	26.1

5.3 Internalization study

The internalization process of ^{99m}Tc-labelled MA peptide based on its binding to VEGFR2 was analyzed in U-87 MG cells. The result of this study demonstrated a notable good and steady rise in internalization of radioligand when the equilibrium between bound

and unbound fraction of [^{99m}Tc]Tc-MA peptide was reached at 90 min (Figure 10), the majority of receptor-bound [^{99m}Tc]Tc-MA peptide was internalized. The time of 90 min, when equilibrium was reached, was considered optimal and was further used in saturation and competitive study.

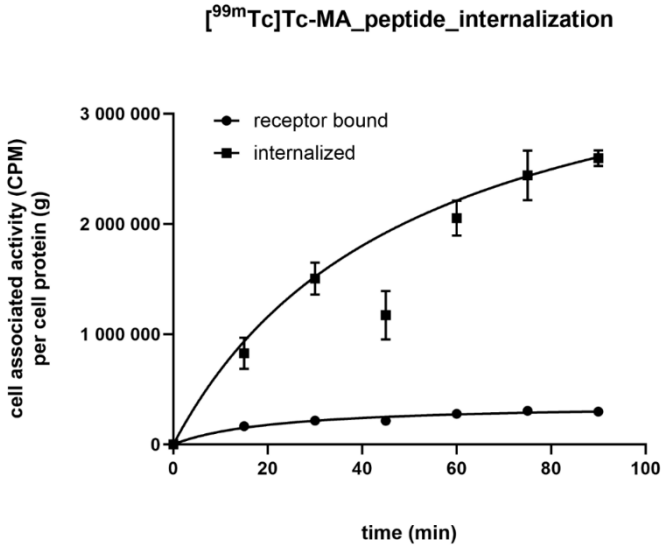

Figure 10 Internalization of [^{99m}Tc]Tc-MA peptide via VEGFR2 presented on the cell surface of U-87 MG cell line. Data are presented as mean ± SD (n=3).

5.4 Saturation and K_D determination

The binding affinity and the equilibrium dissociation constant (K_D) of ^{99m}Tc-labelled MA peptide binding to VEGFR2 expressed in U-87 MG cells were determined by treating cells with increasing concentration of radiolabelled peptide. The final saturation binding curve of [^{99m}Tc]Tc-MA peptide to VEGFR2 from three independent measurements is demonstrated in Figure 11. The equilibrium between the bound and unbound fraction of radioligand was reached at its concentration of 720 nM. The final calculated equilibrium dissociation constant was K_D =103.2 ± 33.7 nM.

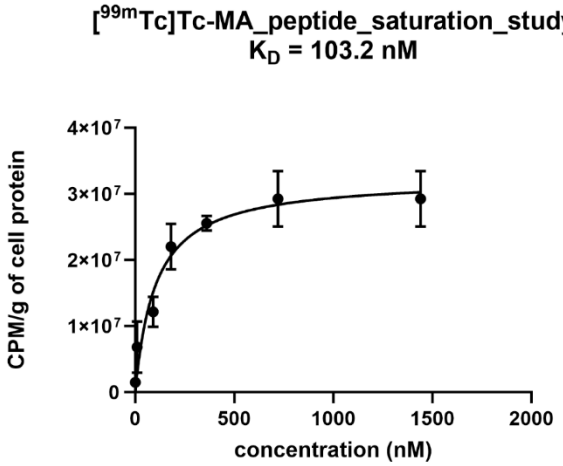

Figure 11 Affinity assessment of ^{99m}Tc-labelled MA peptide in U-87 MG cell line by saturation binding analysis rendered K_D = 103.2 ±33.7 nM. Increasing concentrations of ^{99m}Tc-labelled MA peptide (x-axis) were added to U-87 MG cells and bound radioactivity (y-axis) was determined. Data are presented as mean ± SD. (n=3)

5.5 The competitive study with IC_{50} value assessment

Competition experiments were conducted to assess the specificity of binding of ^{99m}Tc-labelled MA peptide to the VEGFR2 presented on U-87 MG cells. The experiment principle is based on the inhibition of radioligand binding by a non-radiolabelled counterpart presented in a medium with increasing concentration. The binding of the radiolabelled peptide to glioma cancer cells decreased in a concentration-dependent manner of the non-radiolabelled peptide increase, leading to a reduction in bound radioactivity (Figure 12). Three independent experiments resulted in the inhibitory curve, which rendered inhibitory concentration at 50 % of [^{99m}Tc]Tc-MA peptide IC_{50} = 3.75 ± 0.07 μM.

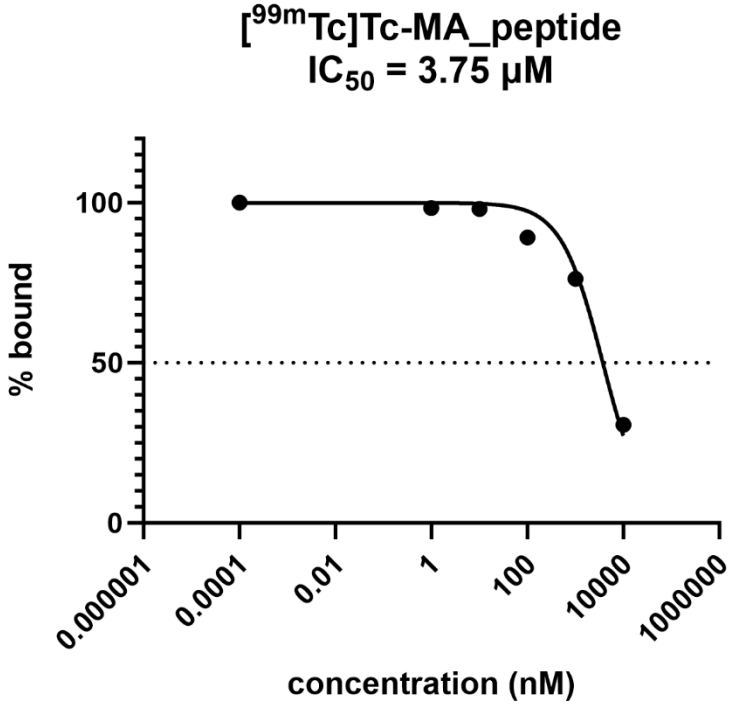

Figure 12 The inhibitory curve of [^{99m}Tc]Tc-MA peptide competing with its non-radiolabelled counterpart MA peptide. The study was performed on the U-87 MG cell line expressing VEGFR2. The result IC_{50} value (IC_{50} = 3.75 ± 0.07 µM) was made from three independent experiments. Data are presented as mean ± SD. (n=3)

6 DISCUSSION

Recent research has focused on utilizing the targeting capabilities of specific molecules to deliver radionuclides directly to tumour sites for imaging and treatment. Effective tumour-targeting drugs should have fast clearance from the bloodstream, a strong affinity for tumour cells, and the ability to stay in the tumour site for an extended period. Peptide- and receptor-mediated approaches to tumour imaging and therapy have gained significant attention in this area (119, 120). Peptides used for receptor-mediated imaging and therapy need to have a strong binding affinity to the tumour and act as antagonists. The VEGF/VEGFR pathway plays a crucial role in tumour angiogenesis and growth and VEGFR2 as a component of this pathway has a key role in tumour angiogenesis which makes it a promising target for cancer imaging and therapy (121, 122). Therefore, in the current study, 18 amino acid MA peptide was synthesized and labelled with technetium-99m for the targeting and imaging of VEGFR2-poitive tumours.

MA peptide was designed based on a work by Basile et al., who introduced a 15 amino acid helical peptide with a sequence of acetyl-KLTWMELYQLAYKGI-amide (denoted in the study as peptide I) as a VEGF receptor antagonist that possesses antiangiogenic biological activity (117). Peptide I was designed on the VEGF N-terminal helix (residue 17-25), and differs only two amino acids from QK that possess defined anti-angiogenic activity (123). However, a half-life of 90 min reported for peptide I remains a challenge and suggests that a protease-resistant analogue could significantly improve the biological effect *in vivo* (117).

In this work, three more amino acids (lysine, aspartic acid, and cysteine) were added to N-terminus peptide I to form an 18 amino acid MA peptide (acetyl-KLTWMELYQLAYKGIKDC-OH). It has been previously demonstrated that incorporating charged amino acids such as lysine, glutamic acid, and aspartic acid onto the N-terminus of proteins at neutral pH can enhance water solubility and facilitate accessibility for chemical modification without significant disruption to the overall protein structure (124). Moreover, the N-terminal α-amine has the unique ability to react in combination with its side chain group, often allowing selective modification through the formation of cyclic intermediates and products (125). Therefore, in the present study cysteine was added as the last N-terminus amino acid of MA peptide. Native chemical ligation (NCL) involves the chemoselective condensation of a thioester with an N-terminal cysteine residue, making it a valuable and versatile tool both for labeling purposes and for the chemical synthesis of large

peptides and proteins (126, 127). In the present study focused on the radiolabelling of MA peptide, MA peptide in about neutral pH was added to a solution containing calcium glucoheptonate with pertechnetate reducing stannous cations ($SnCl_2$). The radiolabelling reaction was performed following the exchange of pre-reduced ^{99m}Tc-glucoheptate with the MA peptide cysteine thiol group as described previously (128).

Labelling of MA peptide with technetium-99m can offer potential SPECT tool for angiogenic process imaging. Technetium-99m has been defined as an interesting imaging agent due to its lasting trapping in the target tissue and rapid clearance from the neighbouring tissues, causing a suitable contrast. In addition, its convenient half-life (τ = 6.6 h) and low but still sufficient energy of emitted gamma rays (144 keV) have always contributed to its favoured imaging application in nuclear medicine (129). ^{99m}Tc-physical-half-life is also convenient due to short biological half-life of peptides including tested MA peptide. Therefore, the choice of appropriate radionuclide for labelling of MA peptide fell on technetium-99m also for that reason of its easy avaibility.

The results of the current study showed that ^{99m}Tc-labelled MA peptide possesses high stability in the mouse serum even reaching 180 min after radiolabelling. The study published by Basille et al. evaluated the stability of the peptide I, when its determined biological half-life was found of about 90 min (118). Interestingly, our results showed that the half-life of ^{99m}Tc-labelled MA peptide increased to more than 180 min, showing that the addition of amino acids lysine, aspartic acid and particularly cysteine to the N-terminus of peptide I could have impact on its stability and prevent its rapid biodegradation (124).

Several types of studies showed that the Cys-tag (sc) motif could be used to radiolabelling with various radionuclides and this fusion tag motif was found to be effective for site-specific protein conjugation without affecting vector functionality. Different radiotracers, including [^{99m}Tc]Tc-scVEGF-PEG-DOTA, [^{99m}Tc]Tc-HYNIC-scVEGF, and [^{64}Cu]Cu-DOTA-PEG-scVEGF, were synthesized and evaluated (130-133). The use of Cys-tag motif in [^{99m}Tc]Tc-HYNIC-C-tagged-VEGF synthesis for tumour vasculature imaging of 4T1 murine tumours was compared with inactivated-VEGF radio-agent. Results showed higher tumour uptake with [^{99m}Tc]Tc-HYNIC-C-tagged-VEGF compared to inactivated-VEGF (134). Furthermore, [^{64}Cu]Cu-DOTA-PEG-scVEGF was found to have more favourable pharmacokinetics in mice compared to [^{99m}Tc]Tc-HYNIC-scVEGF, although both tracers showed detectable but heterogeneous tumour accumulation (135).

The results of internalization showed that after 90 minutes, the majority of receptor-bound [^{99m}Tc]Tc-MA peptide was internalized. Therefore, the time of 90 min was chosen for further evaluation in the saturation and competitive study. The results of calculating equilibrium dissociation constant of ^{99m}Tc-labelled MA peptide binding to VEGFR2 expressed in U-87 MG cells was K_D = 103.2 nM. Comparing our result to those reported in other studies suggests a high found binding affinity of the prepared radioligand to VEGFR2. For example, in the study by Razazadeh et al., two different $_D$(LPR) analogues as ^{99m}Tc-peptide 1 and ^{99m}Tc-peptide 2 were designed for tumour imaging targeting VEGFR1. Their results showed that the K_D value for ^{99m}Tc-peptide 1 and ^{99m}Tc-peptide 2 was 56.8 nM and 71.6 nM, respectively, suggesting that these labelled peptides have high binding affinity to VEGFR1, verified by high tumour accumulation in HT-29 tumor-bearing nude mice (136). Another type of study by Barta et al., showed that ^{68}Ga-labelled peptides, [^{68}Ga]Ga-NODAGA–peptide 1 and [^{68}Ga]Ga-NODAGA–peptide 2, targeting VEGFR had K_D values in the range of 0.5-1.2 μM for human glioblastoma and kidney carcinoma cells (103). Compared to our found K_D value for [^{99m}Tc]Tc-MA peptide, ^{68}Ga-labelled peptides demonstrated 5-10 times worse binding ability.

In addition to equilibrium dissociation constant, inhibitory concentration at 50 % was also calculated in the present study to determine the affinity of ^{99m}Tc-labelled MA peptide binding to VEGFR2. The obtained results showed that ^{99m}Tc-labelled MA peptide had the IC_{50} value equal to 3.75 μM. Our found IC_{50} value is almost comparable to IC_{50} values observed for peptide-induced inhibition of recombinant neuropilins (24 μM) (137) or VEGF165 biological effects (0.8 μM) (138). The IC_{50} values in the range of 3.0–5.6 μM were also reported for [^{68}Ga]Ga-NODAGA–peptide 1 and [^{68}Ga]Ga-NODAGA–peptide 2, suggesting them as potent receptor binding agents which makes them suitable as imaging agents in this study (103).

This study successfuly demonstrated the potential of ^{99m}Tc-labelled MA peptide as a promising agent for tumour imaging of VEGFR2-positive tumours. However, several limitations must be considered. First, the stability of the ^{99m}Tc-labelled MA peptide was primarily evaluated in mouse serum and there is a need for further validation in *in vivo* i.e. in the real organism environment to confirm its stability. This study also relied on a single type of tumour glioblastoma cells (U-87 MG), and the performance of the peptide in other tumour types remains to be explored. In addition, *in vivo* biodistribution and SPECT imaging of the radiolabelled peptide in animal xenografts remains to be investigated. Finally, while the SPECT radioligand labelled MA peptide form showed promising binding ability, the

evaluation of the MA form labelled with therapeutical radionuclide could be worth of further investigation.

7 CONCLUSION

a) The current study successfully radiolabelled the 18-amino acid MA peptide with technetium-99m intended for VEGFR2-positive tumours imaging.

b) The optimalization ^{99m}Tc-labelling process of MA peptide achieved 100% radiochemical purity, which was approved by HPLC analysis with radiometric detection.

c) The presence of cysteine in the N-terminus of MA peptide significantly improved the peptide's stability, when [^{99m}Tc]Tc-MA peptide showed high stability in mouse serum with the biological half-life up to 180 min.

d) The results of internalization discovered that after 90 min, the majority of receptor-bound [^{99m}Tc]-MA peptide was internalized in human glioblastoma cells.

e) The ^{99m}Tc-labelled MA peptide demonstrated its high binding affinity to VEGFR2, with the K_D and IC_{50} values of 103.2 nM and 3.75 μM, respectively, performed in U-87 MG cells.

f) Taken together, these findings suggest that the ^{99m}Tc-labelled MA peptide could be considered as an effective agent in tumor imaging. However, further studies are needed to validate these findings in diverse tumor cell models and in mouse xenografts.

8 ABBREVIATIONS USED

Abbreviation	Meaning of abbreviation
Akt	Protein kinase B (PKB)
ATCC	American Type Culture Collection
bFGF	basic fibroblast growth factor
BM	Basement membrane
BCA	Bicinchoninic acid
cAMP	3′-5′-cyclic adenosine monophosphate
DAG	Diacylglycerol
DMEM	Dulbecco's Modified Eagle Medium
EMT	Epithelial-to-mesenchymal transition
ECM	Extracellular matrix
EGF	Epidermal growth factor
EMA	European Medicines Agency
eNOS	Endothelial NOS
FDA	Food and Drug Administration
FAK	Focal adhesion kinase
FBS	Fetal Bovine Serum
GBM	Glioblastoma multiform
Grb-2	Growth factor receptor-bound protein 2,
HIF	Hypoxia-inducible transcription factor
IP3	Inositol triphosphate
IC_{50}	Inhibitory concentration of 50%
JMD	Juxtamembrane domain
K_D	Dissociation constants
MAPK	Mitogen-activated protein kinase
NRP-1	Neuropilins-1
NRP-2	Neuropilins-2
NSCLC	Nonsquamous cell lung carcinoma
NMPA	National Medical Products Administration
NCL	Native chemical ligation
PlGF	Placenta growth factor
PI3K	Phosphoinositide 3-kinases
PLC-γ	Phospholipase C-γ
PIP2	Phosphatidylinositol 4,5-bisphosphate
PKC	Protein kinase C
PDGFR-α	Platelet-derived growth factor receptor alpha
PD-1	Programmed cell death protein 1
PD-L1	Programmed death-ligand 1
PET	positron emission tomography
PBS	Phosphate-buffered saline
RTKs	Receptor tyrosine kinases
SMIs	Small molecule inhibitors
SNPs	Single-nucleotide polymorphisms
SPECT	Single photon emission tomography
TKD	Tyrosine kinase domain
TNF-α	Tumour necrosis factor-alpha

TGF-α	Transforming growth factor alpha
TGF-β	Transforming growth factor-beta
VPF	Vascular permeability factor
VEGF	Vascular endothelial growth factor
VEGFRs	Vascular endothelial growth factor receptors
VEGFR2	VEGF receptor type 2
99mTc	Technetium-99m

9 THE LIST OF TABLES

10 THE LIST OF FIGURES

11 REFERENCES

1. Cao Y, Langer R, Ferrara N. Targeting angiogenesis in oncology, ophthalmology and beyond. Nature Reviews Drug Discovery. 2023;22(6):476-95.
2. Hunter J. The Works of John Hunter, FRS: Cambridge University Press; 2015.
3. Folkman J. Tumor angiogenesis: therapeutic implications. N Engl j Med. 1971;285(21):1182-6.
4. Karamysheva A. Mechanisms of angiogenesis. Biochemistry (Moscow). 2008;73:751-62.
5. Schmidt A, Brixius K, Bloch W. Endothelial precursor cell migration during vasculogenesis. Circulation research. 2007;101(2):125-36.
6. Herszényi L, Barabás L, Hritz I, István G, Tulassay Z. Impact of proteolytic enzymes in colorectal cancer development and progression. World J Gastroenterol. 2014;20(37):13246-57.
7. Herszényi L, Plebani M, Carraro P, De Paoli M, Roveroni G, Cardin R, et al. Proteases in gastrointestinal neoplastic diseases. Clin Chim Acta. 2000;291(2):171-87.
8. Polgár L. Common feature of the four types of protease mechanism. Biol Chem Hoppe Seyler. 1990;371 Suppl:327-31.
9. Koch AE, Distler O. Vasculopathy and disordered angiogenesis in selected rheumatic diseases: rheumatoid arthritis and systemic sclerosis. Arthritis Res Ther. 2007;9 Suppl 2(Suppl 2):S3.
10. Rajabi M, Mousa SA. The Role of Angiogenesis in Cancer Treatment. Biomedicines. 2017;5(2):34.
11. Madu CO, Wang S, Madu CO, Lu Y. Angiogenesis in Breast Cancer Progression, Diagnosis, and Treatment. J Cancer. 2020;11(15):4474-94.
12. Nishida N, Yano H, Nishida T, Kamura T, Kojiro M. Angiogenesis in cancer. Vasc Health Risk Manag. 2006;2(3):213-9.
13. Bottaro DP, Liotta LA. Cancer: Out of air is not out of action. Nature. 2003;423(6940):593-5.
14. Nelson AR, Fingleton B, Rothenberg ML, Matrisian LM. Matrix metalloproteinases: biologic activity and clinical implications. J Clin Oncol. 2000;18(5):1135-49.
15. Researching Angiogenesis in Cancer: News-Medical.Net 2019 [Available from: https://www.news-medical.net/whitepaper/20190318/Researching-Angiogenesis-in-Cancer.aspx.
16. Awada A, de Castro G, Jr. An integrated approach for tailored treatment in breast cancer. Ann Oncol. 2005;16 Suppl 2:ii203-8.
17. Charmsaz S, Collins DM, Perry AS, Prencipe M. Novel strategies for cancer treatment: highlights from the 55th IACR annual conference. MDPI; 2019.
18. Ichihara E, Kiura K, Tanimoto M. Targeting angiogenesis in cancer therapy. Acta Medica Okayama. 2011;65(6):353-62.
19. Liu Z-L, Chen H-H, Zheng L-L, Sun L-P, Shi L. Angiogenic signaling pathways and anti-angiogenic therapy for cancer. Signal Transduction and Targeted Therapy. 2023;8(1):198.
20. Ghosh S, Sullivan CA, Zerkowski MP, Molinaro AM, Rimm DL, Camp RL, et al. High levels of vascular endothelial growth factor and its receptors (VEGFR-1, VEGFR-2, neuropilin-1) are associated with worse outcome in breast cancer. Human pathology. 2008;39(12):1835-43.
21. Simiantonaki N, Taxeidis M, Jayasinghe C, Kirkpatrick CJ. Epithelial expression of VEGF receptors in colorectal carcinomas and their relationship to metastatic status. Anticancer research. 2007;27(5A):3245-50.
22. Huang H, Held-Feindt J, Buhl R, Mehdorn HM, Mentlein R. Expression of VEGF and its receptors in different brain tumors. Neurological research. 2005;27(4):371-7.
23. Zhao Y, Adjei AA. Targeting Angiogenesis in Cancer Therapy: Moving Beyond Vascular Endothelial Growth Factor. The Oncologist. 2015;20(6):660-73.
24. DiSalvo J, Bayne ML, Conn G, Kwok PW, Trivedi PG, Soderman DD, et al. Purification and Characterization of a Naturally Occurring Vascular Endothelial Growth Factor· Placenta Growth Factor Heterodimer (∗). Journal of Biological Chemistry. 1995;270(13):7717-23.
25. Ferrara N, Carver-Moore K, Chen H, Dowd M, Lu L, O'Shea KS, et al. Heterozygous embryonic lethality induced by targeted inactivation of the VEGF gene. Nature. 1996;380(6573):439-42.

26. Rapisarda A, Melillo G. Role of the VEGF/VEGFR Axis in Cancer Biology and Therapy. In: Daar IO, editor. Advances in Cancer Research. 114: Academic Press; 2012. p. 237-67.
27. Ferrara N, Davis-Smyth T. The biology of vascular endothelial growth factor. Endocrine reviews. 1997;18(1):4-25.
28. Kendall RL, Wang G, DiSalvo J, Thomas KA. Specificity of vascular endothelial cell growth factor receptor ligand binding domains. Biochemical and biophysical research communications. 1994;201(1):326-30.
29. Yang X, Zhang Y, Hosaka K, Andersson P, Wang J, Tholander F, et al. VEGF-B promotes cancer metastasis through a VEGF-A–independent mechanism and serves as a marker of poor prognosis for cancer patients. Proceedings of the National Academy of Sciences. 2015;112(22):E2900-E9.
30. Wu Y, Hooper AT, Zhong Z, Witte L, Bohlen P, Rafii S, et al. The vascular endothelial growth factor receptor (VEGFR-1) supports growth and survival of human breast carcinoma. International journal of cancer. 2006;119(7):1519-29.
31. Mylona E, Alexandrou P, Giannopoulou I, Liapis G, Sofia M, Keramopoulos A, et al. The prognostic value of vascular endothelial growth factors (VEGFs)-A and-B and their receptor, VEGFR-1, in invasive breast carcinoma. Gynecologic oncology. 2007;104(3):557-63.
32. Fan F, Wey JS, McCarty MF, Belcheva A, Liu W, Bauer TW, et al. Expression and function of vascular endothelial growth factor receptor-1 on human colorectal cancer cells. Oncogene. 2005;24(16):2647-53.
33. Lesslie D, Summy J, Parikh N, Fan F, Trevino J, Sawyer T, et al. Vascular endothelial growth factor receptor-1 mediates migration of human colorectal carcinoma cells by activation of Src family kinases. British journal of cancer. 2006;94(11):1710-7.
34. Larcher F, Franco M, Bolontrade M, Rodriguez-Puebla M, Casanova L, Navarro M, et al. Modulation of the angiogenesis response through Ha-ras control, placenta growth factor, and angiopoietin expression in mouse skin carcinogenesis. Molecular Carcinogenesis: Published in cooperation with the University of Texas MD Anderson Cancer Center. 2003;37(2):83-90.
35. Carmeliet P, Moons L, Luttun A, Vincenti V, Compernolle V, De Mol M, et al. Synergism between vascular endothelial growth factor and placental growth factor contributes to angiogenesis and plasma extravasation in pathological conditions. Nature medicine. 2001;7(5):575-83.
36. McColl BK, Baldwin ME, Roufail S, Freeman C, Moritz RL, Simpson RJ, et al. Plasmin activates the lymphangiogenic growth factors VEGF-C and VEGF-D. The Journal of experimental medicine. 2003;198(6):863-8.
37. Hicklin DJ, Ellis LM. Role of the vascular endothelial growth factor pathway in tumor growth and angiogenesis. Journal of clinical oncology. 2005;23(5):1011-27.
38. Calvani M, Rapisarda A, Uranchimeg B, Shoemaker RH, Melillo G. Hypoxic induction of an HIF-1α–dependent bFGF autocrine loop drives angiogenesis in human endothelial cells. Blood. 2006;107(7):2705-12.
39. Smith NR, Baker D, James NH, Ratcliffe K, Jenkins M, Ashton SE, et al. Vascular endothelial growth factor receptors VEGFR-2 and VEGFR-3 are localized primarily to the vasculature in human primary solid cancers. Clinical Cancer Research. 2010;16(14):3548-61.
40. Youssoufian H, Hicklin DJ, Rowinsky EK. monoclonal antibodies to the vascular endothelial growth factor receptor-2 in cancer therapy. Clinical cancer research. 2007;13(18):5544s-8s.
41. Shibuya M, Claesson-Welsh L. Signal transduction by VEGF receptors in regulation of angiogenesis and lymphangiogenesis. Experimental cell research. 2006;312(5):549-60.
42. Haiko P, Makinen T, Keskitalo S, Taipale J, Karkkainen MJ, Baldwin ME, et al. Deletion of vascular endothelial growth factor C (VEGF-C) and VEGF-D is not equivalent to VEGF receptor 3 deletion in mouse embryos. Molecular and cellular biology. 2008;28(15):4843-50.
43. Carmeliet P, De Smet F, Loges S, Mazzone M. Branching morphogenesis and antiangiogenesis candidates: tip cells lead the way. Nature reviews Clinical oncology. 2009;6(6):315-26.
44. Petrova TV, Bono P, Holnthoner W, Chesnes J, Pytowski B, Sihto H, et al. VEGFR-3 expression is restricted to blood and lymphatic vessels in solid tumors. Cancer cell. 2008;13(6):554-6.
45. He Y, Rajantie I, Ilmonen M, Makinen T, Karkkainen MJ, Haiko P, et al. Preexisting lymphatic endothelium but not endothelial progenitor cells are essential for tumor lymphangiogenesis and lymphatic metastasis. Cancer research. 2004;64(11):3737-40.

46. Snuderl M, Batista A, Kirkpatrick ND, de Almodovar CR, Riedemann L, Walsh EC, et al. Targeting placental growth factor/neuropilin 1 pathway inhibits growth and spread of medulloblastoma. Cell. 2013;152(5):1065-76.
47. Nilsson MB, Robichaux J, Herynk MH, Cascone T, Le X, Elamin Y, et al. Altered regulation of HIF-1α in naive-and drug-resistant EGFR-mutant NSCLC: implications for a vascular endothelial growth factor-dependent phenotype. Journal of Thoracic Oncology. 2021;16(3):439-51.
48. Peng X-H, Karna P, Cao Z, Jiang B-H, Zhou M, Yang L. Cross-talk between epidermal growth factor receptor and hypoxia-inducible factor-1α signal pathways increases resistance to apoptosis by up-regulating survivin gene expression. Journal of Biological Chemistry. 2006;281(36):25903-14.
49. Phillips RJ, Mestas J, Gharaee-Kermani M, Burdick MD, Sica A, Belperio JA, et al. Epidermal growth factor and hypoxia-induced expression of CXC chemokine receptor 4 on non-small cell lung cancer cells is regulated by the phosphatidylinositol 3-kinase/PTEN/AKT/mammalian target of rapamycin signaling pathway and activation of hypoxia inducible factor-1α. Journal of Biological Chemistry. 2005;280(23):22473-81.
50. Zhong H, Chiles K, Feldser D, Laughner E, Hanrahan C, Georgescu M-M, et al. Modulation of hypoxia-inducible factor 1α expression by the epidermal growth factor/phosphatidylinositol 3-kinase/PTEN/AKT/FRAP pathway in human prostate cancer cells: implications for tumor angiogenesis and therapeutics. Cancer research. 2000;60(6):1541-5.
51. Melder R, Koenig G, Witwer B, Safabakhsh N, Munn L, Jain R. During angiogenesis, vascular endothelial growth factor and basic fibroblast growth factor regulate natural killer cell adhesion to tumor endothelium. Nature medicine. 1996;2(9):992-7.
52. Kawasaki K, Watabe T, Sase H, Hirashima M, Koide H, Morishita Y, et al. Ras signaling directs endothelial specification of VEGFR2+ vascular progenitor cells. The Journal of cell biology. 2008;181(1):131-41.
53. Matsumoto T, Claesson-Welsh L. VEGF receptor signal transduction. Science's STKE. 2001;2001(112):re21-re.
54. Patel SA, Nilsson MB, Le X, Cascone T, Jain RK, Heymach JV. Molecular Mechanisms and Future Implications of VEGF/VEGFR in Cancer Therapy. Clinical Cancer Research. 2023;29(1):30-9.
55. Beck B, Driessens G, Goossens S, Youssef KK, Kuchnio A, Caauwe A, et al. A vascular niche and a VEGF–Nrp1 loop regulate the initiation and stemness of skin tumours. Nature. 2011;478(7369):399-403.
56. Nilsson MB, Giri U, Gudikote J, Tang X, Lu W, Tran H, et al. KDR Amplification Is Associated with VEGF-Induced Activation of the mTOR and Invasion Pathways but does not Predict Clinical Benefit to the VEGFR TKI Vandetanib. Clin Cancer Res. 2016;22(8):1940-50.
57. Bhattacharya R, Fan F, Wang R, Ye X, Xia L, Boulbes D, et al. Intracrine VEGF signalling mediates colorectal cancer cell migration and invasion. Br J Cancer. 2017;117(6):848-55.
58. Yang F, Tang X, Riquelme E, Behrens C, Nilsson MB, Giri U, et al. Increased VEGFR-2 gene copy is associated with chemoresistance and shorter survival in patients with non-small-cell lung carcinoma who receive adjuvant chemotherapy. Cancer Res. 2011;71(16):5512-21.
59. Zhang L, Wang H, Li C, Zhao Y, Wu L, Du X, et al. VEGF-A/Neuropilin 1 Pathway Confers Cancer Stemness via Activating Wnt/β-Catenin Axis in Breast Cancer Cells. Cell Physiol Biochem. 2017;44(3):1251-62.
60. Elaimy AL, Guru S, Chang C, Ou J, Amante JJ, Zhu LJ, et al. VEGF-neuropilin-2 signaling promotes stem-like traits in breast cancer cells by TAZ-mediated repression of the Rac GAP β2-chimaerin. Sci Signal. 2018;11(528).
61. Wang X, Bove AM, Simone G, Ma B. Molecular Bases of VEGFR-2-Mediated Physiological Function and Pathological Role. Front Cell Dev Biol. 2020;8:599281.
62. Guryanov I, Tennikova T, Urtti A. Peptide Inhibitors of Vascular Endothelial Growth Factor A: Current Situation and Perspectives. Pharmaceutics. 2021;13(9).
63. Le Boeuf F, Houle F, Huot J. Regulation of vascular endothelial growth factor receptor 2-mediated phosphorylation of focal adhesion kinase by heat shock protein 90 and Src kinase activities. Journal of Biological Chemistry. 2004;279(37):39175-85.
64. Gerber H-P, McMurtrey A, Kowalski J, Yan M, Keyt BA, Dixit V, et al. Vascular endothelial growth factor regulates endothelial cell survival through the phosphatidylinositol 3′-kinase/Akt signal

transduction pathway: requirement for Flk-1/KDR activation. Journal of Biological Chemistry. 1998;273(46):30336-43.
65. Murga M, Fernandez-Capetillo O, Tosato G. Neuropilin-1 regulates attachment in human endothelial cells independently of vascular endothelial growth factor receptor-2. Blood. 2005;105(5):1992-9.
66. Masłowska K, Halik PK, Tymecka D, Misicka A, Gniazdowska E. The Role of VEGF Receptors as Molecular Target in Nuclear Medicine for Cancer Diagnosis and Combination Therapy. Cancers. 2021;13(5):1072.
67. Gerber H-P, Kowalski J, Sherman D, Eberhard DA, Ferrara N. Complete inhibition of rhabdomyosarcoma xenograft growth and neovascularization requires blockade of both tumor and host vascular endothelial growth factor. Cancer research. 2000;60(22):6253-8.
68. Escudier B, Bellmunt J, Négrier S, Bajetta E, Melichar B, Bracarda S, et al. Phase III trial of bevacizumab plus interferon alfa-2a in patients with metastatic renal cell carcinoma (AVOREN): final analysis of overall survival. J Clin Oncol. 2010;28(13):2144-50.
69. Friedman HS, Prados MD, Wen PY, Mikkelsen T, Schiff D, Abrey LE, et al. Bevacizumab alone and in combination with irinotecan in recurrent glioblastoma. Journal of clinical oncology. 2009;27(28):4733-40.
70. Kreisl TN, Kim L, Moore K, Duic P, Royce C, Stroud I, et al. Phase II trial of single-agent bevacizumab followed by bevacizumab plus irinotecan at tumor progression in recurrent glioblastoma. Journal of clinical oncology. 2009;27(5):740.
71. Van Meter ME, Kim ES. Bevacizumab: current updates in treatment. Current opinion in oncology. 2010;22(6):586-91.
72. Keunen O, Johansson M, Oudin A, Sanzey M, Rahim SAA, Fack F, et al. Anti-VEGF treatment reduces blood supply and increases tumor cell invasion in glioblastoma. Proceedings of the National Academy of Sciences. 2011;108(9):3749-54.
73. Spratlin J. Ramucirumab (IMC-1121B): Monoclonal antibody inhibition of vascular endothelial growth factor receptor-2. Current oncology reports. 2011;13(2):97-102.
74. Van Cutsem E, Tabernero J, Lakomy R, Prenen H, Prausová J, Macarulla T, et al. Addition of aflibercept to fluorouracil, leucovorin, and irinotecan improves survival in a phase III randomized trial in patients with metastatic colorectal cancer previously treated with an oxaliplatin-based regimen. J Clin Oncol. 2012;30(28):3499-506.
75. Raymond E, Dahan L, Raoul J-L, Bang Y-J, Borbath I, Lombard-Bohas C, et al. Sunitinib malate for the treatment of pancreatic neuroendocrine tumors. New England Journal of Medicine. 2011;364(6):501-13.
76. Llovet JM, Ricci S, Mazzaferro V, Hilgard P, Gane E, Blanc J-F, et al. Sorafenib in advanced hepatocellular carcinoma. New England journal of medicine. 2008;359(4):378-90.
77. Sternberg CN, Davis ID, Mardiak J, Szczylik C, Wagstaff J, Salman P, et al. Pazopanib in locally advanced or metastatic renal cell carcinoma: results of a randomized phase III trial. Journal of clinical oncology. 2010.
78. Patel SA, Nilsson MB, Le X, Cascone T, Jain RK, Heymach JV. Molecular Mechanisms and Future Implications of VEGF/VEGFR in Cancer Therapy. Clin Cancer Res. 2023;29(1):30-9.
79. Wang L, Liu WQ, Broussy S, Han B, Fang H. Recent advances of anti-angiogenic inhibitors targeting VEGF/VEGFR axis. Front Pharmacol. 2023;14:1307860.
80. Moon B-H, Kim Y, Kim S-Y. Twenty Years of Anti-Vascular Endothelial Growth Factor Therapeutics in Neovascular Age-Related Macular Degeneration Treatment. International Journal of Molecular Sciences. 2023;24(16):13004.
81. Fischer C, Jonckx B, Mazzone M, Zacchigna S, Loges S, Pattarini L, et al. Anti-PlGF inhibits growth of VEGF (R)-inhibitor-resistant tumors without affecting healthy vessels. Cell. 2007;131(3):463-75.
82. Shojaei F, Ferrara N. Role of the microenvironment in tumor growth and in refractoriness/resistance to anti-angiogenic therapies. Drug Resistance Updates. 2008;11(6):219-30.
83. Batchelor TT, Sorensen AG, di Tomaso E, Zhang W-T, Duda DG, Cohen KS, et al. AZD2171, a pan-VEGF receptor tyrosine kinase inhibitor, normalizes tumor vasculature and alleviates edema in glioblastoma patients. Cancer cell. 2007;11(1):83-95.

84. Crawford Y, Kasman I, Yu L, Zhong C, Wu X, Modrusan Z, et al. PDGF-C mediates the angiogenic and tumorigenic properties of fibroblasts associated with tumors refractory to anti-VEGF treatment. Cancer cell. 2009;15(1):21-34.
85. Kerbel RS. Tumor angiogenesis. New England Journal of Medicine. 2008;358(19):2039-49.
86. Winkler F, Kozin SV, Tong RT, Chae S-S, Booth MF, Garkavtsev I, et al. Kinetics of vascular normalization by VEGFR2 blockade governs brain tumor response to radiation: role of oxygenation, angiopoietin-1, and matrix metalloproteinases. Cancer cell. 2004;6(6):553-63.
87. Jain RK. Antiangiogenic therapy for cancer: current and emerging concepts. Oncology (Williston Park, NY). 2005;19(4 Suppl 3):7-16.
88. Rust R, Gantner C, Schwab ME. Pro- and antiangiogenic therapies: current status and clinical implications. Faseb j. 2019;33(1):34-48.
89. García-Quintanilla L, Luaces-Rodríguez A, Gil-Martínez M, Mondelo-García C, Maroñas O, Mangas-Sanjuan V, et al. Pharmacokinetics of Intravitreal Anti-VEGF Drugs in Age-Related Macular Degeneration. Pharmaceutics. 2019;11(8).
90. Zhang Y, He B, Liu K, Ning L, Luo D, Xu K, et al. A novel peptide specifically binding to VEGF receptor suppresses angiogenesis in vitro and in vivo. Signal Transduction and Targeted Therapy. 2017;2(1):17010.
91. Shoari A, Khodabakhsh F, Cohan RA, Salimian M, Karami E. Anti-angiogenic peptides application in cancer therapy; a review. Research in Pharmaceutical Sciences. 2021;16(6):559-74.
92. Murukesh N, Dive C, Jayson GC. Biomarkers of angiogenesis and their role in the development of VEGF inhibitors. Br J Cancer. 2010;102(1):8-18.
93. Dowlati A, Gray R, Sandler AB, Schiller JH, Johnson DH. Cell Adhesion Molecules, Vascular Endothelial Growth Factor, and Basic Fibroblast Growth Factor in Patients with Non–Small Cell Lung Cancer Treated with Chemotherapy with or without Bevacizumab—an Eastern Cooperative Oncology Group Study. Clinical Cancer Research. 2008;14(5):1407-12.
94. Schneider BP, Wang M, Radovich M, Sledge GW, Badve S, Thor A, et al. Association of vascular endothelial growth factor and vascular endothelial growth factor receptor-2 genetic polymorphisms with outcome in a trial of paclitaxel compared with paclitaxel plus bevacizumab in advanced breast cancer: ECOG 2100. J Clin Oncol. 2008;26(28):4672-8.
95. Wedam SB, Low JA, Yang SX, Chow CK, Choyke P, Danforth D, et al. Antiangiogenic and antitumor effects of bevacizumab in patients with inflammatory and locally advanced breast cancer. J Clin Oncol. 2006;24(5):769-77.
96. Zhang X, Feng S, Liu J, Li Q, Zheng L, Xie L, et al. Novel small peptides derived from VEGF125-136: potential drugs for radioactive diagnosis and therapy in A549 tumor-bearing nude mice. Scientific Reports. 2017;7(1):4278.
97. Cai W, Hong H. Peptoid and Positron Emission Tomography: an Appealing Combination. Am J Nucl Med Mol Imaging. 2011;1(1):76-9.
98. Christoforidis JB, Williams MM, Kothandaraman S, Kumar K, Epitropoulos FJ, Knopp MV. Pharmacokinetic properties of intravitreal I-124-aflibercept in a rabbit model using PET/CT. Current eye research. 2012;37(12):1171-4.
99. Hao G, Hajibeigi A, León-Rodríguez LM, Oz OK, Sun X. Peptoid-based PET imaging of vascular endothelial growth factor receptor (VEGFR) expression. Am J Nucl Med Mol Imaging. 2011;1(1):65-75.
100. Lu X, Wang RF. A concise review of current radiopharmaceuticals in tumor angiogenesis imaging. Curr Pharm Des. 2012;18(8):1032-40.
101. Rezazadeh F, Sadeghzadeh N, Abedi SM, Abediankenari S. (99m)Tc labeled (D)(LPR): A novel retro-inverso peptide for VEGF receptor-1 targeted tumor imaging. Nucl Med Biol. 2018;62-63:54-62.
102. Giordano RJ, Cardó-Vila M, Salameh A, Anobom CD, Zeitlin BD, Hawke DH, et al. From combinatorial peptide selection to drug prototype (I): targeting the vascular endothelial growth factor receptor pathway. Proceedings of the National Academy of Sciences. 2010;107(11):5112-7.
103. Barta P, Kamaraj R, Kucharova M, Novy Z, Petrik M, Bendova K, et al. Preparation, In Vitro Affinity, and In Vivo Biodistribution of Receptor-Specific 68Ga-Labeled Peptides Targeting Vascular Endothelial Growth Factor Receptors. Bioconjugate Chemistry. 2022;33(10):1825-36.

104. Liu W, Ma H, Li F, Cai H, Liang R, Chen X, et al. PET imaging of VEGFR and integrins in glioma tumor xenografts using 89Zr labelled heterodimeric peptide. Bioorganic & Medicinal Chemistry. 2022;59:116677.
105. Jin F, Krzyzanski W. Pharmacokinetic model of target-mediated disposition of thrombopoietin. AAPS PharmSci. 2004;6(1):E9.
106. Wiley HS, Cunningham DD. The endocytotic rate constant. A cellular parameter for quantitating receptor-mediated endocytosis. J Biol Chem. 1982;257(8):4222-9.
107. Vainshtein I, Roskos LK, Cheng J, Sleeman MA, Wang B, Liang M. Quantitative measurement of the target-mediated internalization kinetics of biopharmaceuticals. Pharm Res. 2015;32(1):286-99.
108. Yang XL, Huang YZ, Xiong WC, Mei L. Neuregulin-induced expression of the acetylcholine receptor requires endocytosis of ErbB receptors. Mol Cell Neurosci. 2005;28(2):335-46.
109. Ren XR, Wei J, Lei G, Wang J, Lu J, Xia W, et al. Polyclonal HER2-specific antibodies induced by vaccination mediate receptor internalization and degradation in tumor cells. Breast Cancer Res. 2012;14(3):R89.
110. Hou P, Araujo E, Zhao T, Zhang M, Massenburg D, Veselits M, et al. B cell antigen receptor signaling and internalization are mutually exclusive events. PLoS Biol. 2006;4(7):e200.
111. Zhu W, Okollie B, Artemov D. Controlled internalization of Her-2/ neu receptors by cross-linking for targeted delivery. Cancer Biol Ther. 2007;6(12):1960-6.
112. Pahara J, Shi H, Chen X, Wang Z. Dimerization drives PDGF receptor endocytosis through a C-terminal hydrophobic motif shared by EGF receptor. Exp Cell Res. 2010;316(14):2237-50.
113. Mazor Y, Barnea I, Keydar I, Benhar I. Antibody internalization studied using a novel IgG binding toxin fusion. J Immunol Methods. 2007;321(1-2):41-59.
114. Carter RE, Sorkin A. Endocytosis of functional epidermal growth factor receptor-green fluorescent protein chimera. J Biol Chem. 1998;273(52):35000-7.
115. Schmidt-Glenewinkel H, Reinz E, Eils R, Brady NR. Systems biological analysis of epidermal growth factor receptor internalization dynamics for altered receptor levels. J Biol Chem. 2009;284(25):17243-52.
116. Kumar SR, Quinn TP, Deutscher SL. Evaluation of an 111In-Radiolabeled Peptide as a Targeting and Imaging Agent for ErbB-2 Receptor–Expressing Breast Carcinomas. Clinical Cancer Research. 2007;13(20):6070-9.
117. Basile A, Del Gatto A, Diana D, Di Stasi R, Falco A, Festa M, et al. Characterization of a designed vascular endothelial growth factor receptor antagonist helical peptide with antiangiogenic activity in vivo. J Med Chem. 2011;54(5):1391-400.
118. Bigott-Hennkens HM, Dannoon S, Lewis MR, Jurisson SS. In vitro receptor binding assays: general methods and considerations. Q J Nucl Med Mol Imaging. 2008;52(3):245-53.
119. Lozza C, Navarro-Teulon I, Pèlegrin A, Pouget JP, Vivès E. Peptides in receptor-mediated radiotherapy: from design to the clinical application in cancers. Front Oncol. 2013;3:247.
120. Majumdar S, Siahaan TJ. Peptide-mediated targeted drug delivery. Med Res Rev. 2012;32(3):637-58.
121. Peng F-W, Liu D-K, Zhang Q-W, Xu Y-G, Shi L. VEGFR-2 inhibitors and the therapeutic applications thereof: a patent review (2012-2016). Expert opinion on therapeutic patents. 2017;27(9):987-1004.
122. Tweedle MF. Peptide-targeted diagnostics and radiotherapeutics. Accounts of chemical research. 2009;42(7):958-68.
123. D'Andrea LD, Iaccarino G, Fattorusso R, Sorriento D, Carannante C, Capasso D, et al. Targeting angiogenesis: structural characterization and biological properties of a de novo engineered VEGF mimicking peptide. Proc Natl Acad Sci U S A. 2005;102(40):14215-20.
124. Rosen CB, Francis MB. Targeting the N terminus for site-selective protein modification. Nature Chemical Biology. 2017;13(7):697-705.
125. Dawson PE, Muir TW, Clark-Lewis I, Kent SB. Synthesis of proteins by native chemical ligation. Science. 1994;266(5186):776-9.
126. Busch GK, Tate EW, Gaffney PR, Rosivatz E, Woscholski R, Leatherbarrow RJ. Specific N-terminal protein labelling: use of FMDV 3C pro protease and native chemical ligation. Chem Commun (Camb). 2008(29):3369-71.
127. Kent SB. Total chemical synthesis of proteins. Chem Soc Rev. 2009;38(2):338-51.

128. Krall N, Pretto F, Mattarella M, Müller C, Neri D. A 99mTc-Labeled Ligand of Carbonic Anhydrase IX Selectively Targets Renal Cell Carcinoma In Vivo. J Nucl Med. 2016;57(6):943-9.
129. Papagiannopoulou D. Technetium-99m radiochemistry for pharmaceutical applications. J Labelled Comp Radiopharm. 2017;60(11):502-20.
130. Backer MV, Levashova Z, Levenson R, Blankenberg FG, Backer JM. Cysteine-containing fusion tag for site-specific conjugation of therapeutic and imaging agents to targeting proteins. Peptide-Based Drug Design. 2008:275-94.
131. Blankenberg FG, Levashova Z, Goris MG, Hamby CV, Backer MV, Backer JM. Targeted systemic radiotherapy with scVEGF/177Lu leads to sustained disruption of the tumor vasculature and intratumoral apoptosis. Journal of Nuclear Medicine. 2011;52(10):1630-7.
132. Levashova Z, Backer M, Hamby CV, Pizzonia J, Backer JM, Blankenberg FG. Molecular imaging of changes in the prevalence of vascular endothelial growth factor receptor in sunitinib-treated murine mammary tumors. Journal of Nuclear Medicine. 2010;51(6):959-66.
133. Wang H, Gao H, Guo N, Niu G, Ma Y, Kiesewetter DO, et al. Site-specific labeling of scVEGF with fluorine-18 for positron emission tomography imaging. Theranostics. 2012;2(6):607.
134. Blankenberg FG, Backer MV, Levashova Z, Patel V, Backer JM. In vivo tumor angiogenesis imaging with site-specific labeled 99m Tc-HYNIC-VEGF. European journal of nuclear medicine and molecular imaging. 2006;33:841-8.
135. Backer MV, Levashova Z, Patel V, Jehning BT, Claffey K, Blankenberg FG, et al. Molecular imaging of VEGF receptors in angiogenic vasculature with single-chain VEGF-based probes. Nature medicine. 2007;13(4):504-9.
136. Rezazadeh F, Sadeghzadeh N, Abedi SM, Abediankenari S. 99mTc labeled D(LPR): A novel retro-inverso peptide for VEGF receptor-1 targeted tumor imaging. Nuclear Medicine and Biology. 2018;62-63:54-62.
137. Perret GY, Starzec A, Hauet N, Vergote J, Le Pecheur M, Vassy R, et al. In vitro evaluation and biodistribution of a 99mTc-labeled anti-VEGF peptide targeting neuropilin-1. Nuclear medicine and biology. 2004;31(5):575-81.
138. Binétruy-Tournaire R, Demangel C, Malavaud B, Vassy R, Rouyre S, Kraemer M, et al. Identification of a peptide blocking vascular endothelial growth factor (VEGF)-mediated angiogenesis. The EMBO journal. 2000.